SMOOTH SLEW MANEUVERS OF FLEXIBLE SPACECRAFT

A THESIS SUBMITTED TO
THE GRADUATE SCHOOL OF NATURAL AND APPLIED SCIENCES
OF
MIDDLE EAST TECHNICAL UNIVERSITY

BY

SÜLEYMAN ALTINIŞIK

IN PARTIAL FULFILLMENT OF THE REQUIREMENTS
FOR
THE DEGREE OF MASTER OF SCIENCE
IN
AEROSPACE ENGINEERING

JANUARY 2019

Approval of the thesis:

SMOOTH SLEW MANEUVERS OF FLEXIBLE SPACECRAFT

submitted by **SÜLEYMAN ALTINIŞIK** in partial fulfillment of the requirements for the degree of **Master of Science in Aerospace Engineering Department, Middle East Technical University** by,

Prof. Dr. Halil Kalıpçılar
Dean, Graduate School of **Natural and Applied Sciences** _____

Prof. Dr. İsmail Hakkı Tuncer
Head of Department, **Aerospace Engineering** _____

Prof. Dr. Ozan Tekinalp
Supervisor, **Aerospace Engineering, METU** _____

Examining Committee Members:

Assist. Prof. Dr. Ali Türker Kutay
Aerospace Engineering, METU _____

Prof. Dr. Ozan Tekinalp
Aerospace Engineering, METU _____

Assist. Prof. Dr. Engin Hasan Çopur
Space and Satellite Engineering, NEU _____

Assist. Prof. Dr. Mohammad Mehdi Gomroki
Aeronautical Engineering, UTAA _____

Assist. Prof. Dr. Kutluk Bilge Arıkan
Mechanical Engineering, TEDU _____

Date: 31.01.2019

I hereby declare that all information in this document has been obtained and presented in accordance with academic rules and ethical conduct. I also declare that, as required by these rules and conduct, I have fully cited and referenced all material and results that are not original to this work.

Name, Surname: Süleyman Altınışık

Signature:

ABSTRACT

SMOOTH SLEW MANEUVERS OF FLEXIBLE SPACECRAFT

Altınışık, Süleyman
Master of Science, Aerospace Engineering
Supervisor: Prof. Dr. Ozan Tekinalp

January 2019, 69 pages

In this thesis, the vibration suppression of flexible spacecraft that carries out attitude tracking maneuvers is addressed. Attitude control algorithm that uses quaternion parametrization is employed. The nonlinear tracking controller employs the to-go quaternion and its derivative. Feedback controller designed is based on this recently developed attitude formulation. Piezoelectric sensors and actuators are also included to rapidly suppress structural vibration. The simulation results demonstrate the success of the algorithm in attitude tracking and vibration suppression.

Keywords: Attitude Tracking, Flexible Spacecraft, Vibration Control, Piezoelectric Actuator, Piezoelectric Sensors, Quaternion, Spacecraft Jitter

ÖZ

ESNEK YAPILI UZAY ARACININ DÜZGÜN YÖNELİM MANEVRALARI

Altınışık, Süleyman
Yüksek Lisans, Havacılık ve Uzay Mühendisliği
Tez Danışmanı: Prof. Dr. Ozan Tekinalp

Ocak 2019, 69 sayfa

Bu tez çalışmasında, yönelim takibi yapan esnek yapılı uzay aracında titreşim önlemesi üzerine çalışılmıştır. Kontrol algoritması yönelim dörtlüğü kullanmaktadır. Doğrusal olmayan takip kontrolcüsü gidilecek yönelim dörtlüğü ve türevini kullanır. Geribildirim kontrolcüsü yeni yönelim formulasyonu kullanılarak tasarlanmıştır. Uzay aracı üzerindeki titreşimleri ortadan kaldırmak için sistemde piezoelektrik algılayıcılar ve eyleyiciler bulunmaktadır. Algoritmanın yönelim takibinde ve titreşim önlemesindeki başarımı benzetim sonuçları ile gösterilmiştir.

Anahtar Kelimeler: Yönelim Takip, Esnek Uzay Aracı, Titreşim Kontolcüsü, Piezoelektrik Eyleyici, Piezoelektrik Algılayıcı, Yönelim Dörtlüğü, Uzay Aracı Titreşimleri

To my family and…all space lovers

ACKNOWLEDGEMENTS

First and foremost, I wish to express my deepest gratitude to my supervisor Prof. Dr. Ozan Tekinalp for his guidance, advice, criticism, encouragements, and insight throughout the research. I owe a very important debt to him.

I am grateful to my fellow colleagues in the department Ali Tevfik Büyükkoçak, Abdurrahim Muratoğlu and Ömer Ataş for their precious help.

I would also like to thank my housemate Mustafa İçen who always kept me entertained with his sense of humor and rambling conversations not only on the thesis but also different aspects of life.

I would especially like to thank my girlfriend Dürdane Çor who has always been by my side supporting me with her kindness, caring and loving support.

Last but not least, I am deeply indebted to my beloved mother, father and sister for their continuous support and encouragement in my time of life.

TABLE OF CONTENTS

LIST OF TABLES

TABLES

LIST OF FIGURES

FIGURES

LIST OF SYMBOLS

SYMBOLS

d	Desired attitude quaternion
q	Spacecraft current attitude quaternion
t	To-go attitude
$\boldsymbol{\omega}$	Angular velocity
S	Strain
σ	Stress
Z	Electric displacement
D	Electric field density
c	Piezoelectric charge constant
Φ	Assumed mode shape
f	Generalized coordinates
ε_i	Permittivity of the piezoelectric material
m_t	Tip mass
θ	Angle of rotation
r	Distance between rigid hub center of mass attachment point
G	Amplifier gain
l	Length of the beam
T	Kinetic energy
J_{mb}	Main body moment of inertia
ρ	Mass per unit length of piezoelectric patch
e_i	Electrode voltage
J	Inertia matrix of whole system
η	Modal coordinate vector

H	Coupling matrix between flexible and rigid dynamics
u	Control torque
$\bar{C}$	Damping matrix
$\bar{K}$	Stiffness matrix
H_2	Coupling matrix between flexible and piezoelectric actuators
u_p	Voltage applied to piezoelectric actuator
ψ	Total velocity of flexible parts
E_t	Total vibration energy
$\mathbf{t}$	Vector part of to-go quaternion
t_4	Scalar part of to-go quaternion
k_p	Proportional gain
k_d	Derivative gain
V	Lyapunov candidate function
Λ_1, Λ_2	Piezoelectric actuator control parameters
$()^x$	Skew-symmetric matrix to carry out vector cross product
λ	Eigen-axis of rotation

CHAPTER 1

INTRODUCTION

Main theme of this thesis is the development of a control algorithm that suppresses vibration in flexible spacecraft on time dependent attitude trajectories. This chapter creates a background about the work by giving an overview of the control problem in flexible spacecraft and by summarizing the contributions made in this work.

In Section 1.1, the flexible spacecraft problem is defined, and the critical aspects of this problem are underlined. The goals of this thesis are explained also in this chapter. In Section 1.2, previously conducted studies on this topic are summarized. Section 1.3 includes the original contributions in this thesis. The chapter concludes with Section 1.4 which presents the organization of the thesis.

1.1 Motivation

In the past five decades, after the travel to the moon in the 20^{th} century, space adventure has gained a great speedup. Developing deep space exploration programs drew attention in many countries. These programs created many new demands in space missions. The growing demands also increased the requirements the satellites must have.

Next generation spacecraft will need a massive amount of electrical energy to accomplish a more complicated mission such as interplanetary missions [1]. Solar panels attached to the satellites may be used to perform such an activity. Then, solar panels must be designed to extend surface to absorb enough sunlight and also they must be lightweight to reduce the cost of the mission. Moreover, today there exists some missions such as Synthetic Aperture Radar satellites with a high amount of

power for its operation (Figure 1.1). This requirement can also be satisfied by producing satellites with a large surface solar panel.

Figure 1.1 Synthetic Aperture Radar Satellites (Left;Sentinel-1, Right; Radarsat-2)

Not only solar panels but also antennas are used in advanced satellites to make a communication with Earth from far away distance. To increase service life and reduce the launch cost, most of the modern satellite often employ large-scale and light damping structures for antennas and solar arrays. This design restriction has become a major challenge recently due to flexibility and vibration effects on spacecraft. These effects may cause many problems in the satellite. Structural failure may be observed due to vibration, or satellite normal operations may be interrupted because of the undesired motion of flexible appendages. An attitude control algorithm that compensates for this vibration and flexibility effects on satellite, is a challenging task. It is not enough to decrease the effect of flexibility with attitude control algorithm. Additionally, these flexible satellites need to achieve attitude maneuver with high pointing precision and stability to perform complex space missions such as Earth observation and space monitoring.

Another challenging task in space missions is the reduction of the sensors and actuators necessary to perform control strategy. Continuation of space missions is a crucial prerequisite. From this point of view, the development of control laws that are capable of fixing such failures is significant. In particular, the modal variables

describing the deflection of flexible elements are crucial for the pointing performance. Moreover, structural tests on Earth may have been considered unreliable because the performance of the controller designed on the basis of perfect knowledge of modal variables may deteriorate in space conditions. As a solution to this problem, dynamic controller or back up controller may be used. Furthermore, although its performance is lower, a dynamic controller is preferable on the grounds that it can be superior to the sensor redundancy policy because it is only based on extra software capabilities on the on-board computer.

Among the active control schemes, piezoelectric actuators have attracted interest as a solution for the attenuation of flexible spacecraft oscillations [2], [3], [4]. There are some studies on these devices that demonstrate its effectiveness to damp out vibration experimentally [5], [6]. Moreover, these devices are lightweight and they also have low power consumption. These devices consist of films of piezoelectric material placed along the flexible parts of the structure (Figure 1.2). Their basic action is to increase the stiffness and the internal damping of the system. Thanks to their inherent distributed nature, they are liable to suppress the vibration of flexible spacecraft.

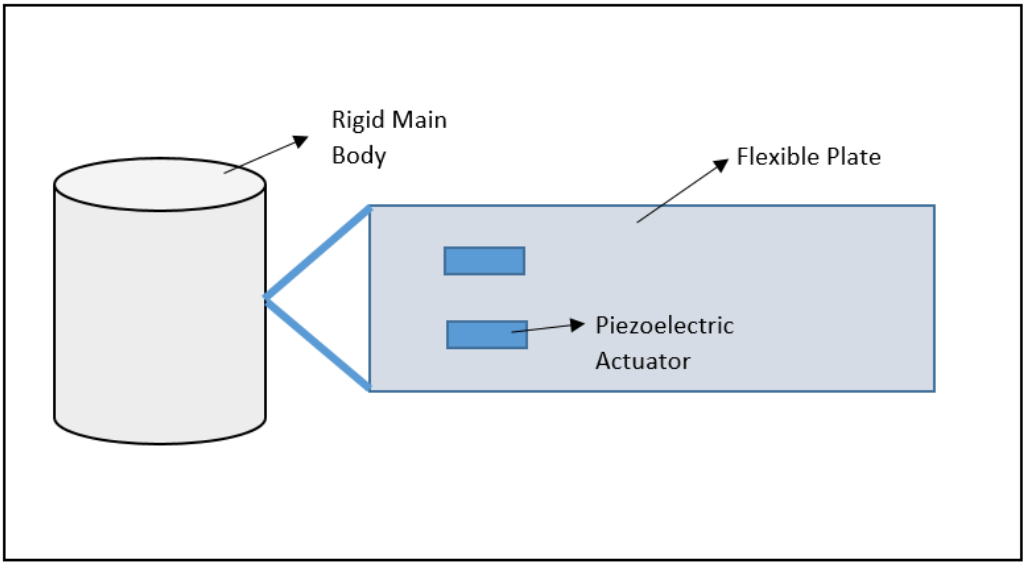

Figure 1.2 Schematic Drawing of Flexible Spacecraft with Piezoelectric Actuators

1.2 Literature Survey

Flexible spacecraft control finds an important area in the control of space systems. There are some books that specifically explain the detail of flexible structures and control of it. The book *Spacecraft Dynamics and Control* by Sidi addresses in detail the problems regarding modeling and control of flexible structures [7]. By using both the Lagrangian approach and extending Hamilton's principle, the flexible spacecraft model with sloshing dynamic may be obtained. Another book *Flexible Spacecraft Dynamics, Control and Guidance* by Mazzini, gives the more detailed model of flexible structure and treats several control methods including Linear Quadratic Regulator and Lyapunov's direct method [8].

Except for books, a number of researchers have studied control of flexible spacecraft. As a control method, the input shaping technique is applied by many researchers [9], [10]. By convoluting a reference input with an impulse sequence, controller attempts to suppress structural vibrations from flexible modes. Although the controller suppresses the vibration effects, the applied technique was developed for linear systems. Therefore its direct application on the nonlinear systems is somewhat limited [11].

Sliding mode control is another control technique applied to flexible spacecraft [12] [13], [14], [15], [16]. It has many advantages like precise tracking, robustness against disturbances and unpredicted inaccuracies. On the other hand, chattering problem that may cause huge damages in the system is the disadvantage of a sliding mode controller.

The attitude control of a spacecraft is a nonlinear problem that requires nonlinear control methods. The most common nonlinear control approach uses a Lyapunov function [17], [18]. Lyapunov stability approach suggests associating an energy-like Lyapunov function to the system. In other words, a function increases as the norm of the system vector increases and decreases as the norm decreases. In order to decide if the function decreases, one can compute the time-derivative of the Lyapunov function

"along the trajectories" of the system to be analyzed. In this theory, the key point is the selection of Lyapunov function. There are no general procedures for choosing a Lyapunov function, which means that there is no unique Lyapunov function for a given system. It is pointed out that Lyapunov's method for a general dynamical system is more of a philosophical approach because of the flexibility in choosing the Lyapunov function [19].

There are some previous works for attitude control of spacecraft which use Lyapunov approach by knowing state of the system totally [20], [21], [22]. These controllers consider that the variables describing the attitude, angular velocity and flexible system elements are measured. Unfortunately, in some cases, due to failure of sensors this is not considered to be known. One way to overcome sensor failure problem could be the use of adaptive control schemes [23], [24], [25]. Another way to achieve this is to use a dynamic controller that compensates the failure of sensors in the spacecraft. Previous works on the design of the dynamic controller may be found in the literature [26], [27], [28], [29].

Another important issue related to control of flexible effect in spacecraft is using the active control schemes. With the advancing technology, many researchers have focused on the problem of active vibration control during the past two decades [30], [31], [32], [33]. For the active vibration control of flexible spacecraft, an effective method is to use the embedded piezoelectric actuators. This is because of the advantages the piezoelectric actuators have. Piezoelectric actuators have high stiffness, lightweight, low power consumption and easy implementation [34], [35].

This thesis aims to propose a flexible spacecraft control method by considering the requirements mentioned above. Nonlinear controller is developed based on Lyapunov stability approach. To increase the fault tolerance of the system, a controller is proposed considering sensor failure in the modal variables and its actuators. Also, active control that uses piezoelectric materials in the system is developed to get a more robust controller.

1.3 Contributions

The contributions of this thesis can be summarized as:

- Designing a novel feedback controller based on recently developed attitude algorithm which takes into account to-go quaternion and its derivative
- Developing an active control method that uses piezoelectric actuator to damp out vibration faster
- Comparing the PD-like(Classical) controller with the tracking controller to observe the effectiveness of the recently developed control algorithm

1.4 Outline

This thesis is structured into the following sections:

In Chapter 1, basic information about flexible spacecraft problem is introduced, and the goals of this thesis are explained. Original contributions made in this thesis are stated. This chapter also includes a review of pertinent literature.

In Chapter 2, the applied attitude dynamic is discussed. Basic information about quaternions are given, and derivation of the attitude controller that takes into account the desired attitude and its derivative is implemented.

In Chapter 3, flexible spacecraft mathematical model is obtained. A rigid satellite and a flexible beam with a tip mass are studied for derivation of the model. Furthermore, mathematical model that contains piezoelectric actuator in the system is given.

In Chapter 4, the development of the control algorithm is performed for different cases. A novel Lyapunov based control algorithm different from the classical PD-like controller is developed. Obtained tracking controller is different from the conventional one because of the new terms in the algorithm. The new algorithm is based on the

attitude formulation that takes time dependent desired attitude and its derivative into account.

In Chapter 5, simulation results for different controllers are given. Firstly, unmodeled dynamic is considered and simulation is performed. Then, considering flexible satellite model simulation is performed. Also, another simulation is conducted adding piezoelectric actuators to the system. All of the simulations are performed for both classical attitude controller and tracking attitude controller. Finally, all the results are compared with each other to show the effectiveness of the tracking controller.

CHAPTER 2

ATTITUDE DYNAMIC PARAMETRIZATION

Quaternion parametrization is used for attitude propagation. It is based on the to-go quaternion formulation that takes the time dependent desired attitude trajectory into account. The derivative of the to-go quaternion is derived.

In section 2.1, brief information about quaternions and quaternion multiplication operator are given. In Section 2.2, derivation of the to-go quaternion is performed and recently developed attitude controller is obtained.

2.1. Quaternions

Quaternions are used for computing three-dimension rotations without any singularity. Its enabling us to describe any rotation in 3-D by an axis of rotation and angle about that axis. Attitude propagation may be parametrized by unit quaternions. A unit quaternion represents a rotation around a unit vector λ, with the amount of angle α. A set of orthogonal *i*, *j*, and *k* may define this axis of rotation,

$$q = \left[\lambda_x \sin\left(\frac{\alpha}{2}\right) \quad \lambda_y \sin\left(\frac{\alpha}{2}\right) \quad \lambda_z \sin\left(\frac{\alpha}{2}\right) \quad \cos\left(\frac{\alpha}{2}\right) \right]^T \tag{2.1}$$

or,

$$q = \lambda_x \sin\left(\frac{\alpha}{2}\right)\boldsymbol{i} + \lambda_y \sin\left(\frac{\alpha}{2}\right)\boldsymbol{j} + \lambda_z \sin\left(\frac{\alpha}{2}\right)\boldsymbol{k} + \cos\left(\frac{\alpha}{2}\right) \tag{2.2}$$

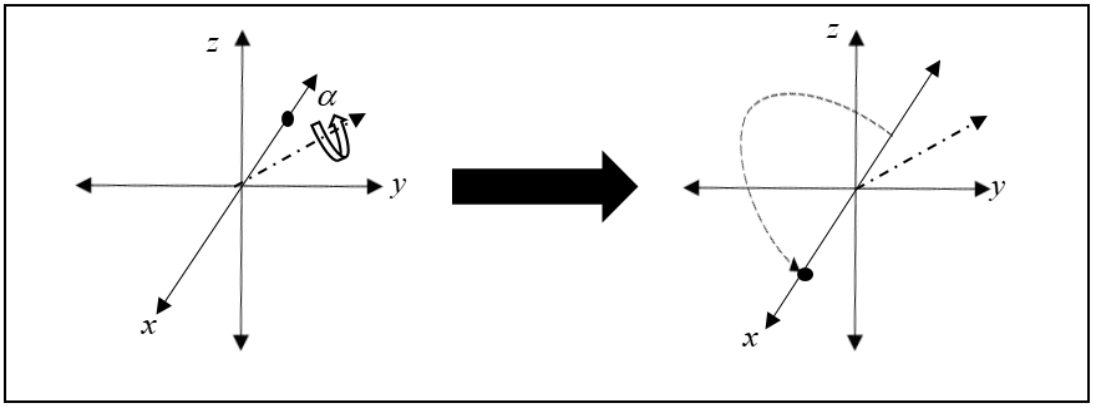

Figure 2.1 Representation of 3-D rotation via Quaternions

A sequence of rotations may be represented by a single quaternion by multiplying them in a special fashion.

$$q \otimes p = q_4\mathbf{p} + p_4\mathbf{q} + \mathbf{q}\times\mathbf{p} + q_4 p_4 - \mathbf{q}^T\mathbf{p} \tag{2.3}$$

where

$$q = (\mathbf{q}, q_4) \tag{2.4}$$

and

$$p = (\mathbf{p}, p_4) \tag{2.5}$$

In the above, $\mathbf{p} = (p_1, p_2, p_3)$ and $\mathbf{q} = (q_1, q_2, q_3)$ are the vector parts of p and q, respectively [8]. Also quaternion multiplication may be written using vector matrix rotation defined in $\mathbb{R}^{4\times4}$ and $\mathbb{R}^{4\times1}$ respectively.

$$q \otimes p = \lfloor q \rceil_{\otimes}\, p \tag{2.6}$$

where,

$$\lfloor q \rceil_{\otimes} = \begin{bmatrix} \mathbf{q}^{x} + q_4 I & \mathbf{q} \\ -\mathbf{q}^T & q_4 \end{bmatrix} \tag{2.7}$$

here, $\mathbf{q}^{\times}$ denotes the skew-symmetric matrix representation of cross product operation.

$$\mathbf{q}^{x}=\begin{bmatrix} 0 & -q_3 & q_2 \\ q_3 & 0 & -q_1 \\ -q_2 & q_1 & 0 \end{bmatrix} \tag{2.8}$$

2.2. Derivation of the To-Go Quaternion

Let define the quaternion associated with the desired attitude using d, and current attitude using q, then the to-go attitude t may be written as [36],

$$d = q \otimes t \tag{2.9}$$

or,

$$t = q^{-1} \otimes d \tag{2.10}$$

where q^{-1} denotes the inverse or conjugate quaternion, since only unit quaternions are considered.

In vector matrix form,

$$\begin{Bmatrix} t_1 \\ t_2 \\ t_3 \\ t_4 \end{Bmatrix} = \begin{bmatrix} -d_4 & -d_3 & d_2 & d_1 \\ d_3 & -d_4 & -d_1 & d_2 \\ -d_2 & d_1 & -d_4 & d_3 \\ d_1 & d_2 & d_3 & d_4 \end{bmatrix} \begin{Bmatrix} q_1 \\ q_2 \\ q_3 \\ q_4 \end{Bmatrix} \tag{2.11}$$

or,

$$\begin{Bmatrix} \mathbf{t} \\ t_4 \end{Bmatrix} = \mathbf{D} \begin{Bmatrix} \mathbf{q} \\ q_4 \end{Bmatrix} \tag{2.12}$$

The derivative of the to-go quaternion may be obtained [36],

$$\begin{Bmatrix} \dot{\mathbf{t}} \\ \dot{t}_4 \end{Bmatrix} = \dot{\mathbf{D}} \begin{Bmatrix} \mathbf{q} \\ q_4 \end{Bmatrix} + \mathbf{D} \begin{Bmatrix} \dot{\mathbf{q}} \\ \dot{q}_4 \end{Bmatrix} \tag{2.13}$$

In general, the desired final attitude is fixed. However, for tracking control the time dependent feature of the desired attitude maybe taken into account [36],

$$\begin{Bmatrix}\dot{\mathbf{q}}\\ \dot{q}_4\end{Bmatrix}=\frac{1}{2}\begin{bmatrix}-\boldsymbol{\omega}^{x} & \boldsymbol{\omega}\\ -\boldsymbol{\omega}^{T} & 0\end{bmatrix}\begin{Bmatrix}\mathbf{q}\\ q_4\end{Bmatrix} \tag{2.14}$$

or,

$$\begin{Bmatrix}\dot{\mathbf{q}}\\ \dot{q}_4\end{Bmatrix}=\frac{1}{2}\boldsymbol{\Omega}\begin{Bmatrix}\mathbf{q}\\ q_4\end{Bmatrix} \tag{2.15}$$

Equation (2.13) may be rewritten as [36],

$$\begin{Bmatrix}\dot{\mathbf{t}}\\ \dot{t}_4\end{Bmatrix}=\dot{\mathbf{D}}\begin{Bmatrix}\mathbf{q}\\ q_4\end{Bmatrix}+\frac{1}{2}\mathbf{D}\boldsymbol{\Omega}\begin{Bmatrix}\mathbf{q}\\ q_4\end{Bmatrix} \tag{2.16}$$

Define the parameter [36],

$$\mathbf{D}_1=\begin{bmatrix}-d_4 & d_3 & -d_2 & d_1\\ -d_3 & -d_4 & d_1 & d_2\\ d_2 & -d_1 & -d_4 & d_3\\ d_1 & d_2 & d_3 & d_4\end{bmatrix} \tag{2.17}$$

and

$$\begin{Bmatrix}\dot{\mathbf{t}}\\ \dot{t}_4\end{Bmatrix}=\left[\dot{\mathbf{D}}\mathbf{D}_1+\frac{1}{2}\mathbf{D}\boldsymbol{\Omega}\mathbf{D}_1\right]\begin{Bmatrix}\mathbf{t}\\ t_4\end{Bmatrix} \tag{2.18}$$

After some simplifications [36],

$$\begin{Bmatrix}\dot{\mathbf{t}}\\ \dot{t}_4\end{Bmatrix}=\left[\begin{bmatrix}\text{-}\boldsymbol{s}^{x} & \boldsymbol{s}\\ \text{-}\boldsymbol{s}^{T} & 0\end{bmatrix}+I\boldsymbol{s}_4+\frac{1}{2}\begin{bmatrix}-\boldsymbol{\omega}^{x} & -\boldsymbol{\omega}\\ \boldsymbol{\omega}^{T} & 0\end{bmatrix}\right]\begin{Bmatrix}\mathbf{t}\\ t_4\end{Bmatrix} \tag{2.19}$$

where,

$$\boldsymbol{s}=\begin{Bmatrix}\dot{d}_1d_4+\dot{d}_2d_3-\dot{d}_3d_2-\dot{d}_4d_1\\ -\dot{d}_1d_3+\dot{d}_2d_4+\dot{d}_3d_1-\dot{d}_4d_2\\ \dot{d}_1d_2-\dot{d}_2d_1+\dot{d}_3d_4-\dot{d}_4d_3\end{Bmatrix},\boldsymbol{s}_4=\dot{d}_1d_1+\dot{d}_2d_2+\dot{d}_3d_3+\dot{d}_4d_4=0 \tag{2.20}$$

and I is the identity matrix. It is easily seen that $\boldsymbol{s}_4=0$ and derivative of the to-go quaternion may be written as [36], [37]

$$\begin{aligned}\dot{\mathbf{t}} &= -(\boldsymbol{s}^{x} + \frac{1}{2}\boldsymbol{\omega}^{x})\mathbf{t} + (\boldsymbol{s} - \frac{1}{2}\boldsymbol{\omega})t_4 \\ \dot{t}_4 &= (-\boldsymbol{s}^{T} + \frac{1}{2}\boldsymbol{\omega}^{T})\mathbf{t}\end{aligned} \tag{2.21}$$

As an attitude controller, Equation (2.21) is used for spacecraft attitude control. As clearly seen, this algorithm takes into account derivative of the desired trajectory.

This algorithm is the extension of the to-go quaternion which may be written as [36], [37], [38],

$$\begin{Bmatrix}\dot{\mathbf{t}} \\ \dot{t}_4\end{Bmatrix} = \frac{1}{2}\begin{bmatrix}\boldsymbol{\omega}^{x} & -\boldsymbol{\omega} \\ \boldsymbol{\omega}^{T} & 0\end{bmatrix}\begin{Bmatrix}\mathbf{t} \\ t_4\end{Bmatrix} \tag{2.22}$$

Also note that the to-go quaternion is the conjugate of the error quaternion commonly used in the literature [17].

CHAPTER 3

MATHEMATICAL MODEL OF A FLEXIBLE SPACECRAFT

This chapter describes the mathematical model of the flexible spacecraft employed in this work. A rigid satellite and a flexible beam with a tip mass is studied. Flexible beam contains bonded piezoelectric material to be used as sensors and actuators.

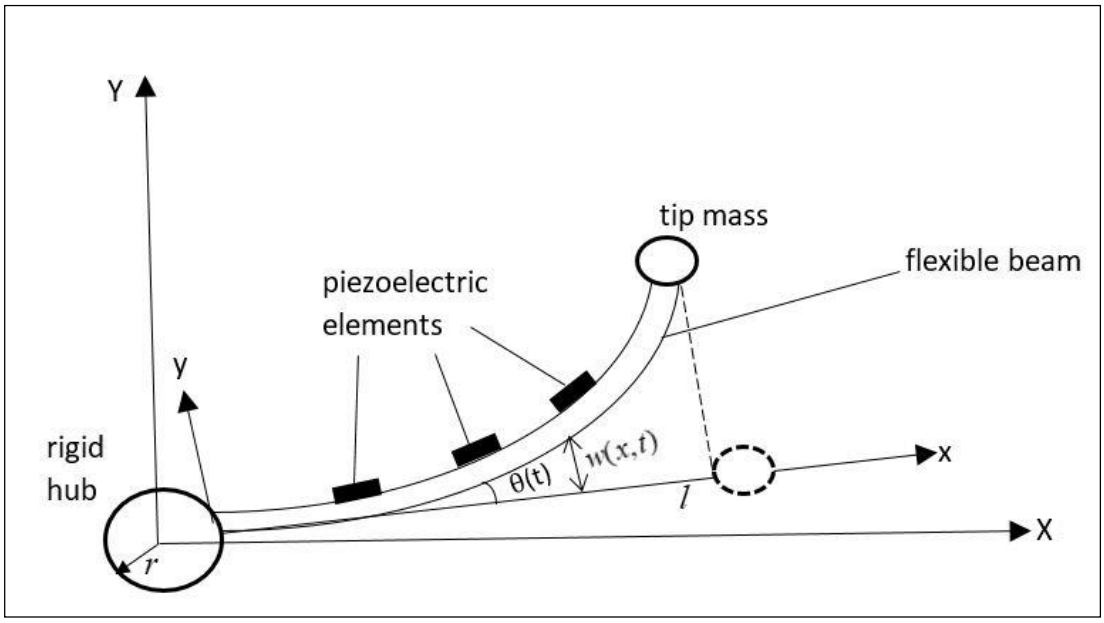

Figure 3.1 Model of Flexible Spacecraft with Bonded Piezoelectric Material

3.1. Constitutive Equation

The linear constitutive equation in a piezoelectric medium may be expressed by the direct and inverse piezoelectric equations respectively. Three-dimensional electromechanical constitutive equation of piezoelectric material can be written as [39],

$$\begin{bmatrix} Z_1 \\ Z_2 \\ Z_3 \\ S_1 \\ S_2 \\ S_3 \\ S_4 \\ S_5 \\ S_6 \end{bmatrix} = \begin{bmatrix} \varepsilon_1^T & 0 & 0 & 0 & 0 & 0 & 0 & c_{15} & 0 \\ 0 & \varepsilon_1^T & 0 & 0 & 0 & 0 & c_{15} & 0 & 0 \\ 0 & 0 & \varepsilon_3^T & c_{31} & c_{31} & c_{33} & 0 & 0 & 0 \\ 0 & 0 & c_{31} & S_{11}^E & S_{12}^E & S_{13}^E & 0 & 0 & 0 \\ 0 & 0 & c_{31} & S_{12}^E & S_{11}^E & S_{13}^E & 0 & 0 & 0 \\ 0 & 0 & c_{33} & S_{13}^E & S_{13}^E & S_{13}^E & 0 & 0 & 0 \\ 0 & c_{15} & 0 & 0 & 0 & 0 & S_{55}^E & 0 & 0 \\ c_{15} & 0 & 0 & 0 & 0 & 0 & 0 & S_{55}^E & 0 \\ 0 & 0 & 0 & 0 & 0 & 0 & 0 & 0 & S_{33}^E \end{bmatrix} \begin{bmatrix} D_1 \\ D_2 \\ D_3 \\ \sigma_1 \\ \sigma_2 \\ \sigma_3 \\ \sigma_4 \\ \sigma_5 \\ \sigma_6 \end{bmatrix} \tag{3.1}$$

where $\sigma_i (i = 1,2,..,6)$ denotes the stress, $S_i (i = 1,2,..,6)$ denotes strain, $Z_i (i = 1,2,..,6)$ denotes the electric displacement along ith axis, $D_i (i = 1,2,3)$ denotes the applied electric field density, $\varepsilon_i (i = 1,2,3)$ denotes the permittivity of the piezoelectric material, $c_{ij} (i = 1,3,\ j = 1,3,5)$ are piezoelectric charge constants and S_{ij}^E are elastic constants of the piezoelectric material.

Strain displacement model of the substructure that is based on Euler-Bernoulli beam theory [35],

$$\varepsilon_x = -y\frac{\partial^2 w}{\partial x^2}, \varepsilon_y = \varepsilon_z = \gamma_{xy} = \gamma_{yz} = \gamma_{zx} = 0 \tag{3.2}$$

Equation (3.1) can be reduced to the one-dimensional constitutive equation with Eqaution (3.2) [35].

$$\begin{Bmatrix} Z_3 \\ S_1 \end{Bmatrix} = \begin{bmatrix} \varepsilon_3^T & c_{31} \\ c_{31} & S_{11}^E \end{bmatrix} \begin{Bmatrix} F_3 \\ T_1 \end{Bmatrix} \tag{3.3}$$

Using the fact that the elastic constant for piezoelectric material is the inverse of its Young's modulus E_p, this equation can be written as [35],

$$\begin{Bmatrix} Z_3 \\ S_1 \end{Bmatrix} = \begin{bmatrix} \varepsilon_3^T - c_{d1}^2 E_p & c_{31} E_P \\ -c_{31} E_P & E_P \end{bmatrix} \begin{Bmatrix} F_3 \\ S_1 \end{Bmatrix} \tag{3.4}$$

3.2. Governing Equation

Several assumptions are made to obtain the model:

1. The beam bends according to the Euler-Bernoulli beam theory
2. The axial deformations and the torsional deformations are neglected.
3. Deformations and strains are small.
4. The piezoelectric layer is homogenous and is unaxially polarized
5. The piezoelectric material is perfectly bonded to the beam

Consider a flexible spacecraft model consisting of a rigid hub in the core and uniform cantilever beam with surface bonded piezoelectric sensors and actuators as shown in Figure 2.1. Also the beam has a tip mass m_t. Define the inertial frames as OXY and the frame fixed on the rigid body as oxy. Then, θ denotes the angle of the rotation along the z axis between these frames.

Based on the satellite model shown in Figure 2.1, total transverse velocity of a mass element on the flexible beam can be computed as follows [40]:

$$v(x,t) = \dot{w}(x,t) + (x+r)\dot{\theta}(t) \tag{3.5}$$

where r be the distance between the rigid hub center of mass and attachment point, x denotes the variable measured from the outer surface of the rigid body along the undeformed axis, $w(x,t)$ is the deflection measured from the x axis.

By using assumed modes method [19], the elastic displacement $w(x,t)$ can be discretized as [35],

$$w(x,t) = \sum_{j=1}^{N} \Phi_j(x) f_j(t) = [\Phi][f] \tag{3.6}$$

where $[\Phi]=[\Phi_1 \quad \Phi_2 \quad ... \quad \Phi_n]$,$[f]=[f_1 \quad f_2 \quad ... \quad f_n]$ state dependent functions $\Phi_j(x)(j=1,...,n)$ are assumed mode shapes or admissible functions which must satisfy the geometric boundary conditions of the problem and $f_j(t)(j=1,...,n)$ are a set of generalized coordinates.

By considering assumptions aforementioned, the total kinetic energy of the active structure can be expressed as [35],

$$T = T_b + \sum_{i=1}^{n_p} T_{pi} \tag{3.7}$$

with,

$$\begin{aligned} T_b = {} & \frac{1}{2} J_h \dot{\theta}^2 + \frac{1}{2} \int_0^l \rho \left[\dot{w} + (r+x)\dot{\theta} \right]^2 dx + \frac{1}{2} \rho \dot{\theta}^2 \int_0^l w^2 dx \\ & + \frac{1}{2} m_t \left[\dot{w}(l,t) + (r+l)\dot{\theta} \right]^2 + \frac{1}{2} m_t w^2(l,t) \dot{\theta}^2 \end{aligned} \tag{3.8}$$

and,

$$T_{pi} = \frac{1}{2} \int_{x_i}^{x_i+h_i} \rho_{pi} \left[\dot{w} + (r+x)\dot{\theta} \right]^2 dx + \frac{1}{2} \rho_{pi} \dot{\theta}^2 \int_{x_i}^{x_i+h_i} w^2 dx \tag{3.9}$$

Where T_b denotes the kinetic energy of substructure, T_{pi} denotes the kinetic energy of the i th piezoelectric patch, n_p denotes the number of piezoelectric patches, l is the length of the beam, J_h is the hub moment of inertia, ρ is the mass per unit length of the piezoelectric patch, ρ_{pi} is the mass per unit length of ith piezoelectric patch, x_i is starting x coordinate of the piezoelectric patch and h_i is the length of the piezoelectric patch.

Also, where the total mass moment of inertia of the beam, hub, tip mass along the z-axis (Figure 3.1) is [35],

$$J = J_h + \int_0^l \rho(r+x)^2 dx + m_t(r+l)^2 + \sum_{i=1}^{n_p} \int_{x_i}^{x_i+h_i} \rho_{pi}(r+x)^2 dx \tag{3.10}$$

$$\begin{aligned}[M] &= \int_0^l \rho[\Phi]^T[\Phi]dx + m_t[\Phi(l)]^T[\Phi(l)] \\ &+ \sum_{i=1}^{n_p} \int_{x_i}^{x_i+h_i} \rho_{pi}[\Phi]^T[\Phi]dx\end{aligned} \tag{3.11}$$

$$\begin{aligned}\left[\tilde{\Phi}\right] &= \int_0^l \rho(r+x)[\Phi]dx + m_t(r+l)^T[\Phi(l)] \\ &+ \sum_{i=1}^{n_p} \int_{x_i}^{x_i+h_i} \rho_{pi}(r+x)[\Phi]dx\end{aligned} \tag{3.12}$$

Then, total kinetic energy can be written as [35],

$$\begin{aligned}T &= \frac{1}{2} J\dot{\theta}^2 + \frac{1}{2}\dot{\theta}^2[f]^T[M][f] + \dot{\theta}[\tilde{\Phi}][\dot{f}] \\ &+ \frac{1}{2}[\dot{f}]^T[M][\dot{f}]\end{aligned} \tag{3.13}$$

Total work done by the system can be given as [35],

$$W = W_b + \sum_{i=1}^{n_p} W_{pi} + W_m \tag{3.14}$$

Where W_b is the work done by the beam, W_{pi} is the work done by the i th piezoelectric patch and W_m is the work done by the external control torque [35].

$$W_b = -\frac{1}{2}\int_0^l E_b I_b \left(\frac{\partial^2 w}{\partial x^2}\right)^2 dx = -\frac{1}{2}[f]^T[K_b][f] \tag{3.15}$$

Where $E_b I_b$ is the flexural rigidity of the beam and K_b is the beam stiffness matrix.

$$[K_b] = \int_0^l E_b I_b [\Phi^{"}]^T [\Phi^{"}] dx \tag{3.16}$$

The work done by the i th piezoelectric patch is the sum of the conservative and non-conservative work terms defined as an integral over the volume of the piezoelectric patches such that [35],

$$\begin{aligned} W_{pi} &= (W_{pi})_c + (W_{pi})_{nc} = \frac{1}{2}\int_{V_i} (-\sigma_{1i} S_{1i} + Z_{3i} D_{3i}) dV_i \\ &= \frac{1}{2} a_{pi} \int_{x_i}^{x_i+h_i} \int_{y_i}^{y_i+h_i} \begin{Bmatrix} Z_{3i} \\ \sigma_{1i} \end{Bmatrix}^T \begin{bmatrix} 1 & 0 \\ 0 & -1 \end{bmatrix} \begin{Bmatrix} D_{3i} \\ \sigma_{1i} \end{Bmatrix} dy dx \end{aligned} \tag{3.17}$$

where y_i is the starting point of the piezoelectric as measured from the neutral axis of the beam and a_{pi} is the width of ith piezoceramic wafer. Using Equation (3.4) and making the notational change $\varepsilon_{xi} = S_{1i}$, Equation (3.17) can be expressed as [35],

$$W_{pi} = \frac{1}{2} a_{pi} \int_{x_i}^{x_i+t_{pi}} \int_{y_i}^{y_i+t_{pi}} \left[(\varepsilon_3^T - c_{31}^2 E_p) D_{3i}^2 + 2 c_{31} E_p D_{3i} \varepsilon_{xi} - E_p \varepsilon_{xi}^2 \right] dy dx \tag{3.18}$$

Using Equation (3.2) and Equation (3.6) and it is assumed that the piezoelectric plates are perfectly bonded to the beam, it can be obtained as [35],

$$W_{pi} = \frac{1}{2} \gamma_i^2 e_i^2 - [f]^T [b_i] e_i - \frac{1}{2} [f]^T [K_{pi}] [f] \tag{3.19}$$

where e_i is the electrode voltage and

$$\gamma_i = \frac{a_{pi} h_i}{t_{pi}} (\varepsilon_3^T - c_{31}^2 E_p), e_i = t_{pi} D_{3i}$$

$$[b_i] = c_{31} E_p a_{pi} \left(y_i + \frac{t_{pi}}{2} \right) \int_{x_i}^{x_i + h_i} [\Phi^{"}]^T dx \tag{3.20}$$

$$[K_{pi}] = a_{pi} t_{pi} E_p \left(y_i^2 + y_i t_{pi} + \frac{t_{pi}^2}{3} \right) \int_{x_i}^{x_i + h_i} [\Phi^{"}]^T [\Phi^{"}] dx$$

The work done by the external torque is given by

$$W_m = u\theta \tag{3.21}$$

Then, substituting Equation (3.15), Equation (3.19) and Equation (3.21) into Equation (3.14), the total work can be written as [35],

$$\begin{aligned} W = & -\frac{1}{2}[e]^T [C][e] - \frac{1}{2}[f]^T [B][e] \\ & -\frac{1}{2}[f]^T [K][f] + T_h \theta \end{aligned} \tag{3.22}$$

where

$$\begin{aligned} [C] &= diag(\gamma_i) \\ [K] &= [K_b] + \sum_{i=1}^{n_p} [K_{pi}] \\ [B] &= \left[(b_1)(b_2)...(b_{n_p}) \right] \\ [e] &= \left[e_1 e_2 ... e_{n_p} \right]^T \end{aligned} \tag{3.23}$$

Using the extended Hamilton's principle, the equations of motion for the spacecraft and flexible appendages with piezoelectric bonded actuators be obtained as [35],

$$J\ddot{\theta} + \ddot{\theta}[f]^T [M][f] + 2\dot{\theta}[f]^T [M][\dot{f}] + \left[\tilde{\Phi} \right][\ddot{f}] = u \tag{3.24}$$

$$\left[\tilde{\Phi} \right]^T \ddot{\theta} + [M][\ddot{f}] + ([K] - \dot{\theta}^2 [M])[f] = -[B][e] \tag{3.25}$$

$$[C][e]=[B]^T[f] \tag{3.26}$$

The general non-linear, time-varying equations of motion for the slewing structure are given in Equations (3.24-3.26). Second order effects may be neglected, if the elastic displacements are small compared to the rigid body rotation. Then, Equation (3.24) can be written as [35],

$$J\ddot{\theta}+[\tilde{\Phi}][\ddot{f}]=u \tag{3.27}$$

Some of the piezoelectric plates will be used as sensors while others will be used as actuators. Then, some of the piezoelectric patches will not have actuator voltage inputs while others will not have sensor voltage outputs. Therefore, $[B]$ and $[C]$ matrices may be broken down in sensor and actuator parts corresponding to the sensor and actuator voltages $[e_s]$ and $[e_a]$. Doing this, Equation (3.25) and Equation (3.26) can be rewritten as [35],

$$[\tilde{\Phi}]^T\ddot{\theta}+[M][\ddot{f}]+[K][f]=-[B_a][G_a][e_a] \tag{3.28}$$

$$[e_s]=[G_s][C_s]^{-1}[B_s]^T[f] \tag{3.29}$$

where $[G_a]$ represents the actuator amplifier gain and $[G_s]$ represents the sensor amplifier gain. The problem of selecting the appropriate locations for the piezoelectric actuators and sensors is a complete problem in itself and thus will not be addressed in this thesis.

Using the following transformation, $[U]^T[M][U]=[I]$ and $[U]^T[K][U]=[\bar{K}]$, which can be solved for the eigenvalues and eigenvectors satisfying the orthonormality conditions, where $[U]$ is a matrix with columns consisting of orthonormal eigenvectors, and $[\bar{K}]=diag(\omega_{ni}^2, i=1,.....N)$ is a matrix with the eigenvalues along the diagonal, and inserting the coordinate transformation $[f]=[U][\eta]$. At the same time, introducing the modal damping, Equation (3.27), Equation (3.28) and Equation (3.29) can be rewritten in terms of modal coordinates [35],

$$J\ddot{\theta}+[H]^T[\ddot{\eta}]=u \tag{3.30}$$

$$[\ddot{\eta}]+[\bar{C}][\dot{\eta}]+[\bar{K}][\eta]+[H]\ddot{\theta}=-[U]^T[B_a][G_a][e_a] \tag{3.31}$$

$$[e_s]=[G_s][C_s]^{-1}[B_s]^T[U][\eta] \tag{3.32}$$

where $[H]^T=[U][\tilde{\Phi}]$ and $[\bar{C}]=diag(2\zeta_i\omega_{ni}, i=1,.....N)$ is modal damping matrix, which ω_i comes from the solution of the eigenvalue problem and normal or experimental value of ζ_i can be used as damping values.

The equation of motion for the flexible spacecraft without piezoelectric elements is given [35],

$$J\ddot{\theta}+[H]^T[\ddot{\eta}]=u \tag{3.33}$$

$$[\ddot{\eta}]+[\bar{C}][\dot{\eta}]+[\bar{K}][\eta]+[H]\ddot{\theta}=0 \tag{3.34}$$

Then, generalized flexible spacecraft dynamic may be obtained as follows:

$$J\dot{\boldsymbol{\omega}}+H^T\ddot{\eta}=u \tag{3.35}$$

and

$$\ddot{\eta}+\bar{C}\dot{\eta}+\bar{K}\eta=-H\dot{\boldsymbol{\omega}} \tag{3.36}$$

where J is the inertia matrix of whole undeformed structure which is symmetric positive definite, η is the modal coordinate vector of flexible modes being considered, H defines the coupling matrix between flexible and rigid dynamics, ω is the angular velocity of the main body and finally u is the control torque to be used. If there are distributed actuators such as piezoelectric actuators, then the equation takes the following form [28]:

$$J\dot{\boldsymbol{\omega}}+H^T\ddot{\eta}=u \tag{3.37}$$

and

$$\ddot{\eta}+\bar{C}\dot{\eta}+\bar{K}\eta=-H\dot{\boldsymbol{\omega}}-H_2u_p \tag{3.38}$$

where H_2 defines the coupling matrix between flexible dynamics and piezoelectric actuators and u_p is the potential differences applied to the piezoelectric actuators and defined as [28],

$$u_p = H_2^T [\Lambda_1 I \quad \Lambda_2 I] \begin{Bmatrix} \eta \\ \psi \end{Bmatrix} \tag{3.39}$$

Then, related equations may be defined as,

$$\begin{aligned} J\dot{\omega} + H^T \ddot{\eta} &= u \\ \ddot{\eta} + \bar{C}\dot{\eta} + \bar{K}\eta &= -H\dot{\omega} \end{aligned} \tag{3.40}$$

and

$$\begin{aligned} J\dot{\omega} + H^T \ddot{\eta} &= u \\ \ddot{\eta} + \bar{C}\dot{\eta} + \bar{K}\eta &= -H\dot{\omega} - H_2 u_p \end{aligned} \tag{3.41}$$

By using Equation (3.40), dynamic of the flexible spacecraft may be obtained in first order form as [28],

$$\begin{aligned} \dot{\omega} &= J_{mb}^{-1}\left[H^T(\bar{C}\psi + \bar{K}\eta - \bar{C}H\omega) + u\right] \\ \dot{\eta} &= \psi - H\omega \\ \dot{\psi} &= -(\bar{C}\psi + \bar{K}\eta - \bar{C}H\omega) \end{aligned} \tag{3.42}$$

with

$$J_{mb} = J - H^T H \tag{3.43}$$

Also $\psi = \dot{\eta} + H\omega$ is total velocity of the flexible beam. Then,

$$\begin{Bmatrix} \dot{\eta} \\ \dot{\psi} \end{Bmatrix} = A \begin{Bmatrix} \eta \\ \psi \end{Bmatrix} - ABH\omega \tag{3.44}$$

where $A = \begin{pmatrix} 0 & I \\ -\bar{K} & -\bar{C} \end{pmatrix}$ and $B = \begin{pmatrix} 0 \\ I \end{pmatrix}$ with the appropriate dimensions.

Also dynamic of the flexible spacecraft with piezoelectric actuator may be obtained by using Equation (3.41),

$$\begin{aligned}\dot{\boldsymbol{\omega}} &= J_{mb}^{-1}\left[H^T(\bar{C}\psi+\bar{K}\eta-\bar{C}H\boldsymbol{\omega})+u+H^T H_2 u_p\right]\\ \dot{\eta} &= \psi - H\boldsymbol{\omega}\\ \dot{\psi} &= -(\bar{C}\psi+\bar{K}\eta-\bar{C}H\boldsymbol{\omega})-H_2 u_p\end{aligned} \tag{3.45}$$

For the sake of simplicity at developing control algorithm, Equation (3.45) may be written as,

$$\dot{\boldsymbol{\omega}} = J_{mb}^{-1}\left[H^T(\bar{C}\psi+\bar{K}\eta-\bar{C}H\boldsymbol{\omega})+u+H^T H_2 u_p\right] \tag{3.46}$$

and,

$$\begin{pmatrix}\dot{\eta}\\ \dot{\psi}\end{pmatrix} = \bar{A}\begin{pmatrix}\eta\\ \psi\end{pmatrix} - ABH\boldsymbol{\omega} \tag{3.47}$$

where $\bar{A} = A - BH_2 H_2^T[\Lambda_1 I \quad \Lambda_2 I] = \begin{pmatrix} 0 & I \\ -(\bar{K}+\Lambda_1 H_2 H_2^T) & -(\bar{C}+\Lambda_2 H_2 H_2^T)\end{pmatrix}$ with the appropriate dimensions.

Also, using the modal coordinates total vibration energy may be written as [35],

$$E_t = \dot{\eta}^T\dot{\eta} + \eta^T\bar{K}\eta \tag{3.48}$$

CHAPTER 4

ATTITUDE CONTROL ALGORITHMS

In this chapter, Lyapunov function based feedback control algorithms are developed. One control algorithm is based on the classic to-go quaternion attitude formulation. Another algorithm uses the recently developed attitude formulation that may smoothly maneuvers on predefined time dependent attitude trajectories. Lyapunov candidate functions are defined based on these attitude formulations. Also, piezoelectric actuators and sensors are also added to improve structural damping properties of the control system. Table that lists the number controllers used are given in Table 4.1.

In Section 4.1, unmodeled flexible dynamic is considered. Control system design is based on rigid body model using its actuators and rigid body sensors. In Section 4.2, discrete flexible body sensors beside rigid body sensors are taken into account. Control system design is based on the flexible satellite model. In Section 4.3, piezoelectric actuators are also added to the system. In all sections, controllers are designed considering two different quaternion based attitude controllers.

Table 4.1 Control System Design

Equation of Motion	**Actuators**	**Sensors**
Rigid Body Equation of Motion	Rigid Body Actuators	Rigid Body Sensors
Flexible Body Equation of Motion	Rigid Body Actuators	Rigid Body Sensors + Discrete Flexible Body Sensors
Flexible Body Equation of Motion	Rigid Body Actuators + Piezoelectric Actuators	Rigid Body Sensors + Discrete Flexible Body Sensors

4.1. Case Study 1: Control Using Rigid Body Actuators and Rigid Body Sensors

In this section, the derivation of the control algorithm is based on the rigid body equations of motion. Rigid body sensors and rigid body actuators are available in the system.

The first requirement is that spacecraft tracks the desired attitude. Consequently, control law must ensure the spacecraft attitude tracks the desired attitude. The second requirement is that the vibration of spacecraft's flexible appendages shall also be damped out.

For the former requirement, quaternions are considered. To-go quaternion basically defines the difference between the desired attitude and realized attitude (i.e. attitude error). The attitude tracking requirement may be formulated such that as time goes to infinity, the vectorial part of to-go attitude must go to zero $\lim_{t\to\infty}\mathbf{t} = 0$ (i.e. $\lim_{t\to\infty} t_4 = 1$)

Latter requirement may be quantified as modal coordinates vector goes to zero $\lim_{t\to\infty}\eta = 0$.

4.1.1. Classical Attitude Controller

In this part, the classical rigid body attitude controller is proposed.

Theorem: The following feedback control law brings the system to desired attitude in a stable fashion.

$$u = k_p \mathbf{t} - k_d \boldsymbol{\omega} \tag{4.1}$$

for $k_p > 0$ and $k_d > 0$ properly selected.

Proof: Consider the following positive definite Lyapunov function:

$$V_1 = 2(k_p)(1-t_4) + \frac{1}{2}\boldsymbol{\omega}^T J_{mb}\boldsymbol{\omega} \tag{4.2}$$

Taking time derivative of Equation (4.2),

$$\dot{V}_1 = -2(k_p)\dot{t}_4 + \boldsymbol{\omega}^T J_{mb}\dot{\boldsymbol{\omega}} \tag{4.3}$$

Equations of motion without flexible body dynamics,

$$\dot{\boldsymbol{\omega}} = J_{mb}^{-1}(-\boldsymbol{\omega}^T J_{mb}\boldsymbol{\omega} + u) \tag{4.4}$$

Substituting Equation (4.4) into the Equation (4.3),

$$\dot{V}_1 = -\boldsymbol{\omega}^T k_d \boldsymbol{\omega} \tag{4.5}$$

is negative definite for $k_p > 0$ and $k_d > 0$.

4.1.2. Effect of Flexible Body Dynamics

To include the effect of flexible body dynamics on the stability, we consider the following Lyapunov equation.

$$V = V_1 + V_2 \tag{4.6}$$

with

$$V_1 = 2(k_p)(1-t_4) + \frac{1}{2}\boldsymbol{\omega}^T J_{mb}\boldsymbol{\omega} \tag{4.7}$$

and

$$V_2 = \frac{1}{2}(\eta^T \quad \psi^T)P_1\begin{pmatrix}\eta\\ \psi\end{pmatrix} \tag{4.8}$$

where $P_1 = P_1^T > 0$

Taking time derivative of Equation (4.6),

$$\dot{V}_1 = -2(k_p)\dot{t}_4 + \boldsymbol{\omega}^T J_{mb}\dot{\boldsymbol{\omega}} \tag{4.9}$$

and

$$\dot{V}_2 = (\eta^T \quad \psi^T)P_1\begin{pmatrix}\dot{\eta}\\ \dot{\psi}\end{pmatrix} \tag{4.10}$$

Substituting Equation (2.22) into the Equation (4.9),

$$\dot{V}_1 = -k_p\omega^T\mathbf{t} + \omega^T J_{mb}\dot{\boldsymbol{\omega}} \tag{4.11}$$

Also substituting Equation (3.42) into the Equation (4.11),

$$\dot{V}_1 = -k_p\boldsymbol{\omega}^T\mathbf{t} + \boldsymbol{\omega}^T\left[H^T(\bar{C}\psi + \bar{K}\eta - \bar{C}H\boldsymbol{\omega}) + u\right] \tag{4.12}$$

and Equation (4.1) into the Equation (4.12),

$$\dot{V}_1 = -\boldsymbol{\omega}^T k_d\boldsymbol{\omega} + \boldsymbol{\omega}^T H^T\left(\bar{C}\psi + \bar{K}\eta - \bar{C}H\boldsymbol{\omega}\right) \tag{4.13}$$

Then substituting Equation (3.44) into the Equation (4.10),

$$\dot{V}_2 = (\eta^T \quad \psi^T)P_1\left[A\begin{pmatrix}\eta\\ \psi\end{pmatrix} - ABH\boldsymbol{\omega}\right] \tag{4.14}$$

Then,

$$\dot{V} = -\boldsymbol{\omega}^T k_d \boldsymbol{\omega} + (\eta^T \quad \psi^T) P_1 A \begin{pmatrix} \eta \\ \psi \end{pmatrix} - (\eta^T \quad \psi^T) P_1 ABH\boldsymbol{\omega} - \boldsymbol{\omega}^T H^T \bar{C} H\boldsymbol{\omega} + \boldsymbol{\omega}^T H^T \left(\bar{C}\psi + \bar{K}\eta\right) \tag{4.15}$$

In Equation (4.15), if k_d is properly selected, derivative of the Lyapunov function will be decaying. Defining the term $\boldsymbol{\omega}^T H^T \left(\bar{C}\psi + \bar{K}\eta\right) = Q_A$. Then, if the attitude and control parameters defined as in Chapter 5, Figure 4.1 shows the values of the term Q_A.

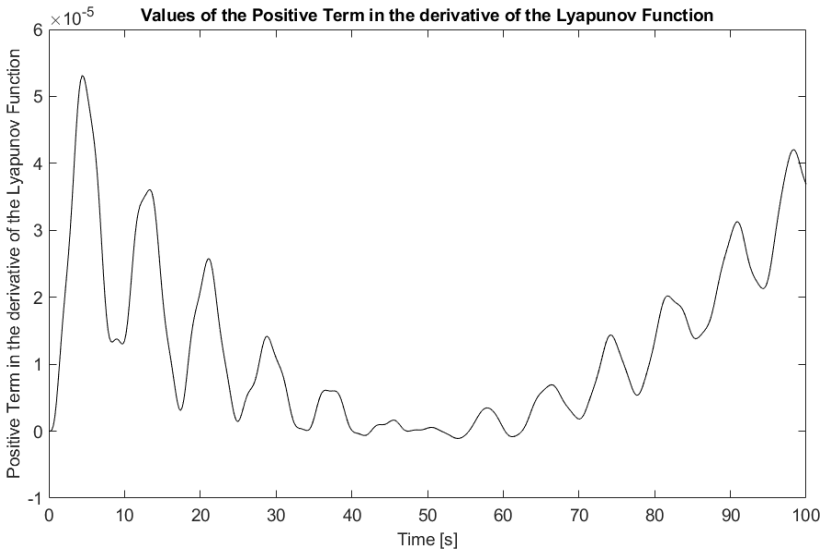

Figure 4.1 Values of the Positive Term (Q_A) in the derivative of the Lyapunov Function when a smooth time dependent slew maneuver is required

Also, including all the terms in Equation (4.15) is simulated. The results are presented in Figure 4.2. From this plot it may be observed that the Lyapunov function derivative never go positive values with the selected k_d

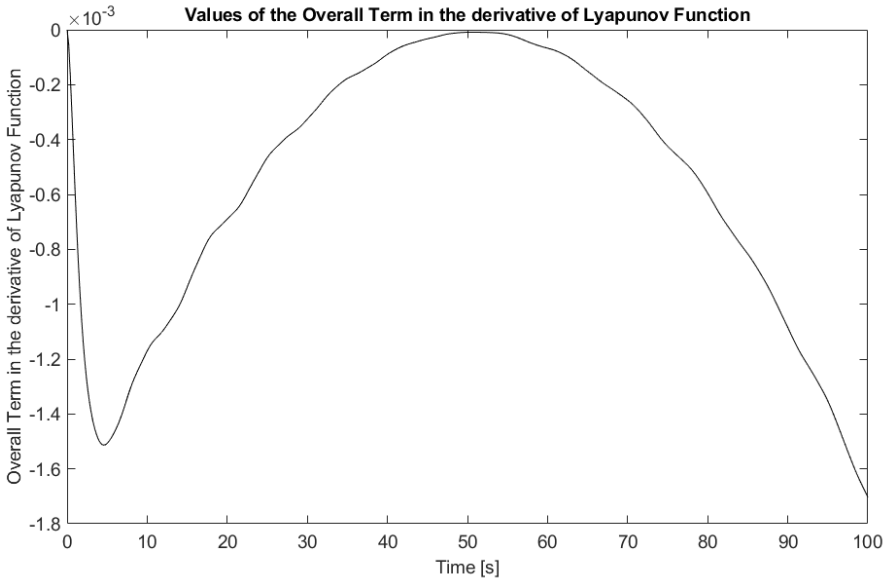

Figure 4.2 The Lyapunov function derivative history when a smooth time dependent slew maneuver is required

Even if stepwise slew maneuver is input, the positive definite part of the Lyapunov function, Q_A is still bounded. Figure 4.3 shows the time history of Q_A and Figure 4.4 shows the total value of the Lyapunov function derivative.

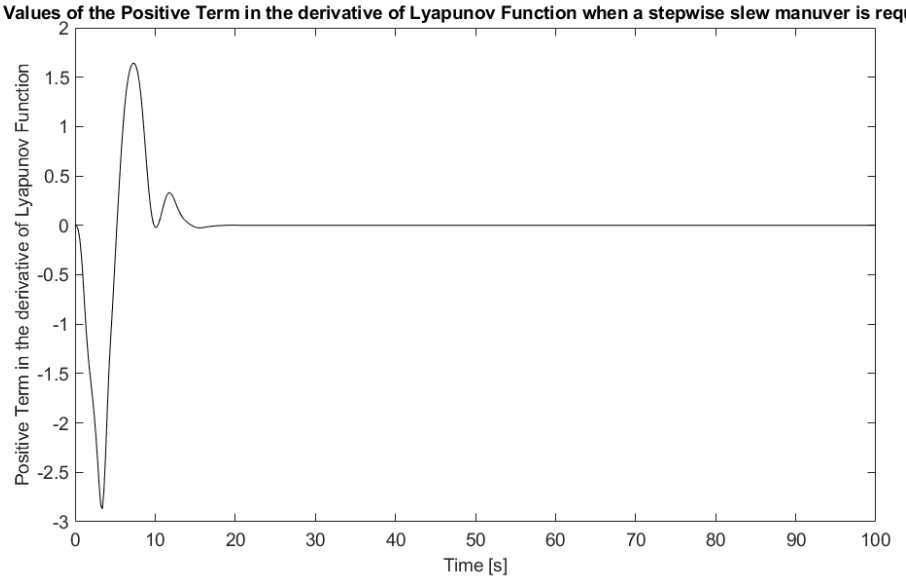

Figure 4.3 Values of the Positive Term (Q_A) in the derivative of the Lyapunov Function when a stepwise slew maneuver is input

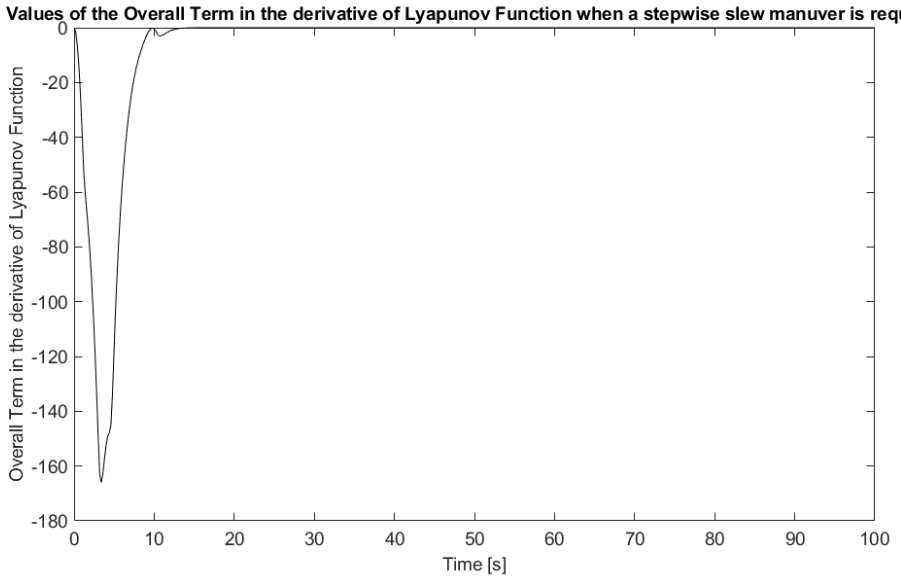

Figure 4.4 The Lyapunov Function derivative history when a stepwise slew maneuver is input

The negative definiteness of the Lyapunov function derivative may also be shown analytically. To show the global stability, derivative may be defined as,

$$\dot{V} = x^T Q_5 x + Q_A \tag{4.16}$$

where $x = (\boldsymbol{\omega}^T \quad \eta^T \quad \psi^T)^T$ is the state vector and,

$$Q_5 = \begin{pmatrix} -k_d I - H^T \bar{C} H & -Q_3^T \\ -Q_3 & -Q_1 \end{pmatrix} \tag{4.17}$$

P_1 may be computed as solution of the Lyapunov equation:

$$-Q_1 = \frac{1}{2}\left[P_1 A + A^T P_1 \right] \tag{4.18}$$

$$Q_3 = \frac{P_1 A B H}{2}$$

Note that Lyapunov stability theorem indicates that given a stable A matrix a positive definite matrix P can be found such that $-Q = PA + A^T P$ where Q is also positive definite [41]. Using the Lyapunov stability theorem, the matrix Q_1 is a fixed positive definite matrix and solution of the P_1 exists because $\sigma(A) \subset \mathbb{C}^-$, with $\sigma(.)$ denoting the set of eigenvalues. Then, the matrix Q_5 is negative definite, $\sigma(Q_5) \subset \mathbb{C}^-$, for a positive k_d.

4.1.3. Tracking Attitude Controller

In this section, recently developed attitude propagation algorithm given in Equation (2.21) is employed. It gives a more precise trajectory tracking solution since the derivative of the desired trajectory is included.

Theorem: The following controller brings the attitude to the desired one asymptotically:

$$u = k_p \mathbf{t} - k_d \boldsymbol{\omega} + 2(k_d \mathbf{s} + J_{mb} \dot{\mathbf{s}}) \tag{4.19}$$

for all $k_p > 0$ and $k_d > 0$ properly selected.

Proof: Given control law may be derived using a properly selected Lyapunov function.

$$V = V_3 + V_2 \tag{4.20}$$

with

$$V_3 = 2k_p(1-t_4) + \frac{1}{2}(-2\boldsymbol{s}+\boldsymbol{\omega})^T J_{mb}(-2\boldsymbol{s}+\boldsymbol{\omega}) \tag{4.21}$$

and

$$V_2 = \frac{1}{2}(\eta^T \quad \psi^T)P_1\begin{pmatrix}\eta\\ \psi\end{pmatrix} \tag{4.22}$$

where $P_1 = P_1^T > 0$

Taking time derivative of Equation (4.20) to show asymptotic stability,

$$\dot{V}_3 = -2(k_p)\dot{t}_4 + (-2\boldsymbol{s}+\boldsymbol{\omega})^T J_{mb}(-2\dot{\boldsymbol{s}}+\dot{\boldsymbol{\omega}}) \tag{4.23}$$

and

$$\dot{V}_2 = (\eta^T \quad \psi^T)P_1\begin{pmatrix}\dot{\eta}\\ \dot{\psi}\end{pmatrix} \tag{4.24}$$

Substituting Equation (2.21) into the Equation (4.23),

$$\dot{V}_3 = -k_p(-2\boldsymbol{s}^T + \boldsymbol{\omega}^T)\mathbf{t} + (-2\boldsymbol{s}+\boldsymbol{\omega})^T J_{mb}(-2\dot{\boldsymbol{s}}+\boldsymbol{\omega}) \tag{4.25}$$

Also substituting Equation (3.42) into the Equation (4.25),

$$\begin{aligned}\dot{V}_3 = &-k_p(-2\boldsymbol{s}^T + \boldsymbol{\omega}^T)\mathbf{t} - (-2\boldsymbol{s}+\boldsymbol{\omega})^T J_{mb}(2\dot{\boldsymbol{s}}) + \\ &(-2\boldsymbol{s}+\boldsymbol{\omega})^T\left[H^T(\bar{C}\psi + \bar{K}\eta - \bar{C}H\boldsymbol{\omega}) + u\right]\end{aligned} \tag{4.26}$$

and Equation (4.19) into the Equation (4.26),

$$\begin{aligned}\dot{V}_3 = &-(-2\boldsymbol{s}+\boldsymbol{\omega})^T k_d(-2\boldsymbol{s}+\boldsymbol{\omega}) + \\ &(-2\boldsymbol{s}+\boldsymbol{\omega})^T H^T\left(\bar{C}\psi + \bar{K}\eta - \bar{C}H\boldsymbol{\omega}\right)\end{aligned} \tag{4.27}$$

Then substituting Equation (3.44) into the Equation (4.24),

$$\dot{V}_2 = (\eta^T \quad \psi^T) P_1 \left[A \begin{pmatrix} \eta \\ \psi \end{pmatrix} - ABH\boldsymbol{\omega} \right] \tag{4.28}$$

Then,

$$\begin{aligned} \dot{V} = & -(-2\boldsymbol{s} + \boldsymbol{\omega})^T k_d (-2\boldsymbol{s} + \boldsymbol{\omega}) + (\eta^T \quad \psi^T) P_1 A \begin{pmatrix} \eta \\ \psi \end{pmatrix} - \\ & (\eta^T \quad \psi^T) P_1 ABH\boldsymbol{\omega} - \boldsymbol{\omega}^T H^T \bar{C} H\boldsymbol{\omega} + \\ & (-2\boldsymbol{s} + \boldsymbol{\omega})^T H^T \left(\bar{C}\psi + \bar{K}\eta \right) + (2\boldsymbol{s})^T H^T \bar{C} H\boldsymbol{\omega} \end{aligned} \tag{4.29}$$

In Equation (4.29), if k_d is properly selected, derivative of the Lyapunov function will be decaying. Defining the term $(-2\boldsymbol{s} + \boldsymbol{\omega})^T H^T \left(\bar{C}\psi + \bar{K}\eta \right) + (2\boldsymbol{s})^T H^T \bar{C} H\boldsymbol{\omega} = Q_B$. Then, if the attitude and control parameters defined as in Chapter 5, Figure 4.5 shows the values of the term Q_B.

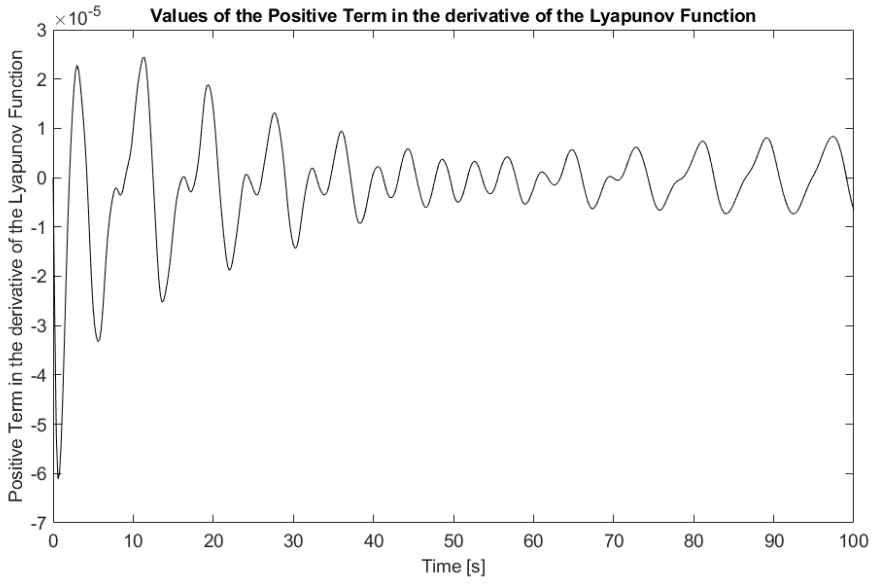

Figure 4.5 Time History of the Positive Term (Q_B) in the derivative of the Lyapunov function when a smooth time dependent slew maneuver is carried out

All terms in Equation (4.29) is plotted in Figure 4.6. The graph shows that the derivative of the Lyapunov function is always positive.

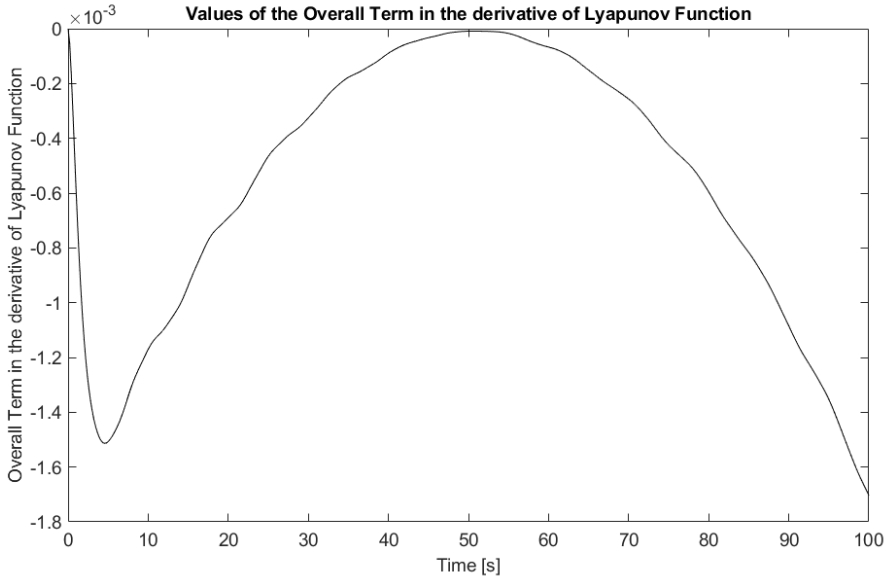

Figure 4.6 Time History of the Lyapunov function derivative when a smooth time dependent slew maneuver is carried out

The negative definiteness of the Lyapunov function may also be proved as follows:

$$\dot{V} = -(2\boldsymbol{s})^T k_d (2\boldsymbol{s}) + x^T Q_5 x + Q_B \tag{4.30}$$

where $x = (\boldsymbol{\omega}^T \quad \eta^T \quad \psi^T)^T$ is state vector with

$$Q_5 = \begin{pmatrix} -k_d I - H^T \bar{C} H & -Q_3^T \\ -Q_3 & -Q_1 \end{pmatrix}$$

$$-Q_1 = \frac{1}{2}\left[P_1 A + A^T P_1 \right] \tag{4.31}$$

$$Q_3 = \frac{P_1 A B H}{2}$$

Using the Lyapunov stability theorem [41], the matrix Q_1 is a fixed positive definite matrix with the P_1 is the solution of Sylvester equation and exists because $\sigma(A) \subset \mathbb{C}^-$, with $\sigma(.)$ denoting the set of eigenvalues. Then, the matrix Q_5 is negative definite, $\sigma(Q_5) \subset \mathbb{C}^-$, for a positive k_d.

4.2. Case Study 2: Using Rigid Body Actuators and Rigid and Flexible Body Sensors

In this case study, derivation of the control algorithm is performed considering flexible body sensors are available in the system.

Control requirements may be defined as in Section 4.1.

4.2.1. Attitude Control Using to-go Quaternion

Theorem: The following controller brings the attitude to the desired one in a stable fashion:

$$u = k_p \mathbf{t} - k_d \boldsymbol{\omega} - H^T \left(\bar{C}\psi + \bar{K}\eta - \bar{C}H\boldsymbol{\omega} \right) \tag{4.32}$$

for $k_p > 0$ and $k_d > 0$ properly selected.

Proof: Consider the following positive definite Lyapunov function:

$$V = V_1 + V_2 \tag{4.33}$$

with

$$V_1 = 2(k_p)(1 - t_4) + \frac{1}{2}\boldsymbol{\omega}^T J_{mb} \boldsymbol{\omega} \tag{4.34}$$

and

$$V_2 = \frac{1}{2}(\eta^T \quad \psi^T) P_1 \begin{pmatrix} \eta \\ \psi \end{pmatrix} \tag{4.35}$$

where $P_1 = P_1^T > 0$

Taking time derivative of Equation (4.33) to show asymptotic stability,

$$\dot{V}_1 = -2(k_p)\dot{t}_4 + \boldsymbol{\omega}^T J_{mb}\dot{\boldsymbol{\omega}} \tag{4.36}$$

and

$$\dot{V}_2 = (\eta^T \quad \psi^T)P_1\begin{pmatrix}\dot{\eta}\\ \dot{\psi}\end{pmatrix} \tag{4.37}$$

Substituting Equation (2.22), Equation (3.42) and Equation (4.32) into the Equation (4.36),

$$\dot{V}_1 = -\boldsymbol{\omega}^T k_d \boldsymbol{\omega} \tag{4.38}$$

Then substituting Equation (3.47) into the Equation (4.37),

$$\dot{V}_2 = (\eta^T \quad \psi^T)P_1\left[A\begin{pmatrix}\eta\\ \psi\end{pmatrix} - ABH\boldsymbol{\omega}\right] \tag{4.39}$$

Then,

$$\dot{V} = -\boldsymbol{\omega}^T k_d \boldsymbol{\omega} + (\eta^T \quad \psi^T)P_1 A\begin{pmatrix}\eta\\ \psi\end{pmatrix} - (\eta^T \quad \psi^T)P_1 ABH\boldsymbol{\omega} \tag{4.40}$$

Then,

$$\dot{V} = x^T Q_6 x \le 0 \tag{4.41}$$

where $x = (\boldsymbol{\omega}^T \quad \eta^T \quad \psi^T)^T$ is the state vector and P_1 may be computed as the solution of the Lyapunov equation as before, and,

$$Q_6 = \begin{pmatrix} -k_d I & -Q_3^T \\ -Q_3 & -Q_1 \end{pmatrix}$$
$$-Q_1 = \frac{1}{2}\left[P_1 A + A^T P_1 \right] \tag{4.42}$$
$$Q_3 = \frac{P_1 ABH}{2}$$

Using the Lyapunov stability theorem as it is stated in Section 4.1.2, the matrix Q_1 is a fixed positive definite matrix and solution of the P_1 exists because $\sigma(A) \subset \mathbb{C}^-$, with $\sigma(.)$ denoting the set of eigenvalues. Then, the matrix Q_6 is negative definite, $\sigma(Q_6) \subset \mathbb{C}^-$, for properly selected k_d.

4.2.2. Attitude Control Using to-go Quaternion with Derivative

Recently developed attitude control algorithm is used for the tracking attitude control given in Equation (2.21). It offers a more precise trajectory tracking solution since derivative of the desired trajectory is taken into account.

Theorem: The following controller brings the attitude to the desired one in a stable fashion:

$$u = k_p \mathbf{t} - k_d \boldsymbol{\omega} + 2(k_d \mathbf{s} + J_{mb}\dot{\mathbf{s}}) - H^T \left(\bar{C}\psi + \bar{K}\eta - \bar{C}H\boldsymbol{\omega} \right) \tag{4.43}$$

for all $k_p > 0$ and $k_d > 0$ properly selected.

Proof: Consider the positive definite Lyapunov function:

$$V = V_3 + V_2 \tag{4.44}$$

with

$$V_3 = 2k_p(1 - t_4) + \frac{1}{2}(-2\mathbf{s} + \boldsymbol{\omega})^T J_{mb}(-2\mathbf{s} + \boldsymbol{\omega}) \tag{4.45}$$

and

$$V_2 = \frac{1}{2}(\eta^T \quad \psi^T)P_1\begin{pmatrix}\eta\\ \psi\end{pmatrix} \tag{4.46}$$

where $P_1 = P_1^T > 0$

Taking time derivative of Equation (4.44) to show asymptotic stability,

$$\dot{V}_3 = -2(k_p)\dot{t}_4 + (-2\boldsymbol{s} + \boldsymbol{\omega})^T J_{mb}(-2\dot{\boldsymbol{s}} + \dot{\boldsymbol{\omega}}) \tag{4.47}$$

and

$$\dot{V}_2 = (\eta^T \quad \psi^T)P_1\begin{pmatrix}\dot{\eta}\\ \dot{\psi}\end{pmatrix} \tag{4.48}$$

Substituting Equation (2.21), Equation (3.42) and Equation (4.43) into the Equation (4.47),

$$\dot{V}_3 = -(-2\boldsymbol{s} + \boldsymbol{\omega})^T k_d(-2\boldsymbol{s} + \boldsymbol{\omega}) \tag{4.49}$$

Then substituting Equation (3.47) into the Equation (4.48),

$$\dot{V}_2 = (\eta^T \quad \psi^T)P_1\left[A\begin{pmatrix}\eta\\ \psi\end{pmatrix} - ABH\boldsymbol{\omega}\right] \tag{4.50}$$

Then,

$$\begin{aligned}\dot{V} = &-(-2\boldsymbol{s} + \boldsymbol{\omega})^T k_d(-2\boldsymbol{s} + \boldsymbol{\omega}) + \\ &(\eta^T \quad \psi^T)P_1 A\begin{pmatrix}\eta\\ \psi\end{pmatrix} - (\eta^T \quad \psi^T)P_1 ABH\boldsymbol{\omega}\end{aligned} \tag{4.51}$$

Then,

$$\dot{V} = -(2\boldsymbol{s})^T k_d(2\boldsymbol{s}) + x^T Q_6 x \tag{4.52}$$

where $x = (\boldsymbol{\omega}^T \quad \eta^T \quad \psi^T)^T$ is state vector with

$$Q_6 = \begin{pmatrix} -k_d I & -Q_3^T \\ -Q_3 & -Q_1 \end{pmatrix}$$
$$-Q_1 = \frac{1}{2}\left[P_1 A + A^T P_1 \right] \tag{4.53}$$
$$Q_3 = \frac{P_1 ABH}{2}$$

Using the Lyapunov stability theorem [41], the matrix Q_1 is a fixed positive definite matrix with the P_1 is the solution of Sylvester equation and exists because $\sigma(\bar{A}) \subset \mathbb{C}^-$, with $\sigma(.)$ denoting the set of eigenvalues. Then, the matrix Q_6 is also negative definite, $\sigma(Q_6) \subset \mathbb{C}^-$, for properly selected k_d.

Thus the controller proposed brings to system to the desired attitude asymptotically.

4.3. Case Study 3: Control with Rigid and Flexible Body Actuators and Rigid and Flexible Body Sensors

In this section, piezoelectric actuators added to the system to damp out vibration effect on the spacecraft faster. Derivation of the control algorithm is performed. Control requirements may be defined as in Section (4.1).

4.3.1. Attitude Control Using to-go Quaternion

Theorem: The following controller brings the attitude to the desired one in a stable fashion:

$$u = k_p \mathbf{t} - k_d \boldsymbol{\omega} - H^T \left(\bar{C}\psi + \bar{K}\eta - \bar{C}H\boldsymbol{\omega} \right) - H^T H_2 u_p \tag{4.54}$$

for $k_p > 0$ and $k_d > 0$ properly selected.

Proof: Given control law may be derived using a properly selected Lyapunov function. Positive definite Lyapunov function:

$$V = V_1 + V_2 \tag{4.55}$$

with

$$V_1 = 2(k_p)(1-t_4) + \frac{1}{2}\boldsymbol{\omega}^T J_{mb}\boldsymbol{\omega} \tag{4.56}$$

and

$$V_2 = \frac{1}{2}(\eta^T \quad \psi^T)P_2\begin{pmatrix}\eta\\ \psi\end{pmatrix} \tag{4.57}$$

where $P_2 = P_2^T > 0$

Taking time derivative of Equation (4.55) to show asymptotic stability,

$$\dot{V}_1 = -2(k_p)\dot{t}_4 + \boldsymbol{\omega}^T J_{mb}\dot{\boldsymbol{\omega}} \tag{4.58}$$

and

$$\dot{V}_2 = (\eta^T \quad \psi^T)P_2\begin{pmatrix}\dot{\eta}\\ \dot{\psi}\end{pmatrix} \tag{4.59}$$

Substituting Equation (2.22), Equation (3.46) and Equation (4.54) into the Equation (4.58),

$$\dot{V}_1 = -\boldsymbol{\omega}^T k_d\boldsymbol{\omega} \tag{4.60}$$

Then substituting Equation (3.47) into the Equation (4.59),

$$\dot{V}_2 = (\eta^T \quad \psi^T)P_2\left[\bar{A}\begin{pmatrix}\eta\\ \psi\end{pmatrix} - ABH\boldsymbol{\omega}\right] \tag{4.61}$$

Then,

$$\dot{V} = -\boldsymbol{\omega}^T k_d\boldsymbol{\omega} + (\eta^T \quad \psi^T)P_2\bar{A}\begin{pmatrix}\eta\\ \psi\end{pmatrix} - (\eta^T \quad \psi^T)P_2 ABH\boldsymbol{\omega} \tag{4.62}$$

or it may be written as,

$$\dot{V} = x^T Q_7 x \leq 0 \tag{4.63}$$

where $x = (\boldsymbol{\omega}^T \quad \eta^T \quad \psi^T)^T$ is the state vector

$$Q_7 = \begin{pmatrix} -k_d I & -Q_4^T \\ -Q_4 & -Q_2 \end{pmatrix} \tag{4.64}$$

P_2 is the solution of the Lyapunov equation:

$$-Q_2 = \frac{1}{2}\left[P_2 \bar{A} + \bar{A}^T P_2 \right] \tag{4.65}$$

$$Q_4 = \frac{P_2 ABH}{2}$$

Using the Lyapunov stability theorem [41], the matrix Q_2 is a fixed positive definite matrix and solution of the P_2 exists because $\sigma(\bar{A}) \subset \mathbb{C}^-$, with $\sigma(.)$ denoting the set of eigenvalues. Then, the matrix Q_7 is negative definite, $\sigma(Q_7) \subset \mathbb{C}^-$, for properly selected k_d, proving asymptotic stability of the proposed controller.

4.3.2. Attitude Control Using to-go Quaternion with Derivative

Recently developed attitude algorithm is used for the attitude controller that may be seen in Equation (2.21).

Theorem: The following controller brings the attitude to the desired one in a stable fashion:

$$u = k_p \mathbf{t} - k_d \boldsymbol{\omega} + 2(k_d \mathbf{s} + J_{mb}\dot{\mathbf{s}}) - H^T \left(\bar{C}\psi + \bar{K}\eta - \bar{C}H\boldsymbol{\omega} \right) - H^T H_2 u_p \tag{4.66}$$

for all $k_p > 0$ and $k_d > 0$ properly selected.

Proof: Given control law may be derived using a properly selected Lyapunov function. Positive definite Lyapunov function:

$$V = V_3 + V_2 \tag{4.67}$$

with

$$V_3 = 2k_p(1-t_4) + \frac{1}{2}(-2\boldsymbol{s}+\boldsymbol{\omega})^T J_{mb}(-2\boldsymbol{s}+\boldsymbol{\omega}) \tag{4.68}$$

and

$$V_2 = \frac{1}{2}(\eta^T \quad \psi^T)P_2\begin{pmatrix}\eta\\ \psi\end{pmatrix} \tag{4.69}$$

where $P_2 = P_2^T > 0$

Taking time derivative of Equation (4.67) to show asymptotic stability,

$$\dot{V}_3 = -2(k_p)\dot{t}_4 + (-2\boldsymbol{s}+\boldsymbol{\omega})^T J_{mb}(-2\dot{\boldsymbol{s}}+\dot{\boldsymbol{\omega}}) \tag{4.70}$$

and

$$\dot{V}_2 = (\eta^T \quad \psi^T)P_2\begin{pmatrix}\dot{\eta}\\ \dot{\psi}\end{pmatrix} \tag{4.71}$$

Substituting Equation (2.21), Equation (3.46) and Equation (4.66) into the Equation (4.70),

$$\dot{V}_3 = -(-2\boldsymbol{s}+\boldsymbol{\omega})^T k_d(-2\boldsymbol{s}+\boldsymbol{\omega}) \tag{4.72}$$

Then substituting Equation (3.47) into the Equation (4.71),

$$\dot{V}_2 = (\eta^T \quad \psi^T)P_2\left[\bar{A}\begin{pmatrix}\eta\\ \psi\end{pmatrix} - ABH\boldsymbol{\omega}\right] \tag{4.73}$$

Then,

$$\dot{V} = -(-2\boldsymbol{s} + \boldsymbol{\omega})^T k_d (-2\boldsymbol{s} + \boldsymbol{\omega}) + (\eta^T \quad \psi^T) P_2 \bar{A} \begin{pmatrix} \eta \\ \psi \end{pmatrix} - (\eta^T \quad \psi^T) P_2 ABH\boldsymbol{\omega} \tag{4.74}$$

or it may be written as,

$$\dot{V} = -(2\boldsymbol{s})^T k_d (2\boldsymbol{s}) + x^T Q_7 x \tag{4.75}$$

where $x = (\boldsymbol{\omega}^T \quad \eta^T \quad \psi^T)^T$ is state vector with

$$Q_7 = \begin{pmatrix} -k_d I & -Q_4^T \\ -Q_4 & -Q_2 \end{pmatrix}$$
$$-Q_2 = \frac{1}{2}\left[P_2 \bar{A} + \bar{A}^T P_2 \right] \tag{4.76}$$
$$Q_4 = \frac{P_2 ABH}{2}$$

Using the Lyapunov stability theorem as it is stated in Section 4.1.1 [41], once the matrix Q_2 is a fixed positive definite matrix with the P_1 is the solution of Sylvester equation and exists because $\sigma(\bar{A}) \subset \mathbb{C}^-$, with $\sigma(.)$ denoting the set of eigenvalues. Then, the matrix Q_7 is negative definite, $\sigma(Q_7) \subset \mathbb{C}^-$, for properly selected k_d. As it derived in Section (4.3.1), we may find that the largest invariant set ε with the help of LaSalle theorem. Then all the control objectives are satisfied.

CHAPTER 5

SIMULATION RESULTS

In this chapter, simulation results for different attitude controllers are presented. There are 3 different cases considered. Simulation of the mathematical model of flexible spacecraft as well as attitude dynamics are developed in MATLAB/Simulink environment.

In Section 5.1, simulation results for the case study 1 is given. Based on the unmodeled flexible dynamics, rigid body model using its sensors and actuators in this simulation. On the other hand, in Section 5.2, discrete flexible body sensors are considered beside rigid body sensors. In Section 5.3, simulations are performed by adding piezoelectric actuators to the system to damp out vibration effect on the spacecraft faster. In all sections, simulations are performed considering two different attitude controllers, where the first one only uses to-go quaternion and the second one that also employs the derivative of the desired attitude.

The desired attitude is defined as a time dependent function. A Cubic function is taken for the rotation angle. By using initial and final conditions, rotation angle coefficients may be obtained. Simulation time is choosen as 100 seconds. Unitary quaternion coefficients are taken for simplicity. Simulation parameters for the attitude are given in Table 5.1.

Table 5.1 Simulation Parameters for Attitude Dynamic

Parameter	**Value**
Desired Attitude	$\begin{Bmatrix} \mathbf{d} \\ d_4 \end{Bmatrix} = \begin{Bmatrix} \lambda \sin(\alpha/2) \\ \cos(\alpha/2) \end{Bmatrix}$
Rotation Angle	$\alpha = a + bt + ct^2 + et^3$
Rotation Angle Initial & Final Conditions	$\alpha_0 = 0 \;\; \dot{\alpha}_0 = 0 \;\; \alpha_f = \frac{2\pi}{3} \;\; \dot{\alpha}_f = 0$
Quaternion Coefficient	$\lambda = (1,2,3)^T / \sqrt{14}$
Final Time	$t_f = 100$ s

By using parameters listed in Table 5.1, the time history for the desired attitude in terms of quaternion parameters may be obtained as in Figure 5.1.

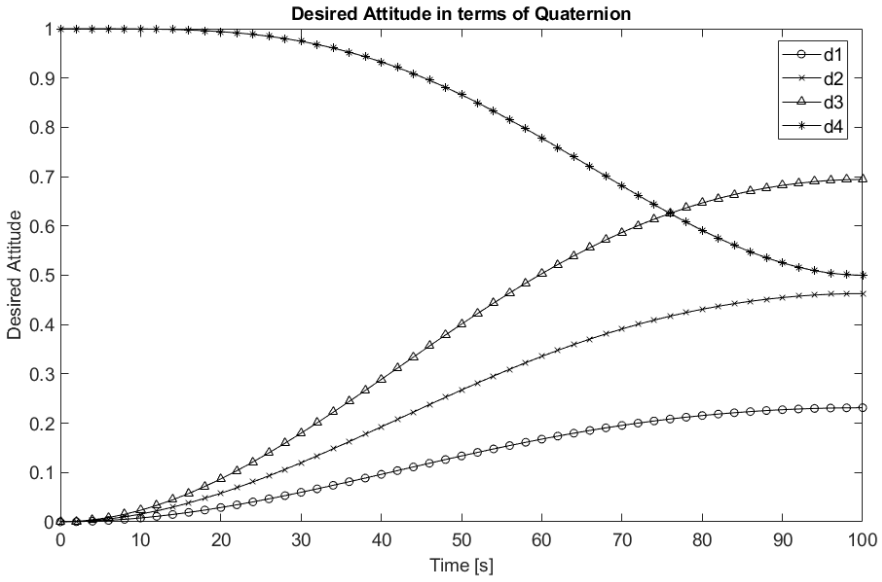

Figure 5.1 Time History of Desired Attitude in terms of Quaternion

Also, time history of desired attitude in terms of Euler angles may be seen in Figure 5.2.

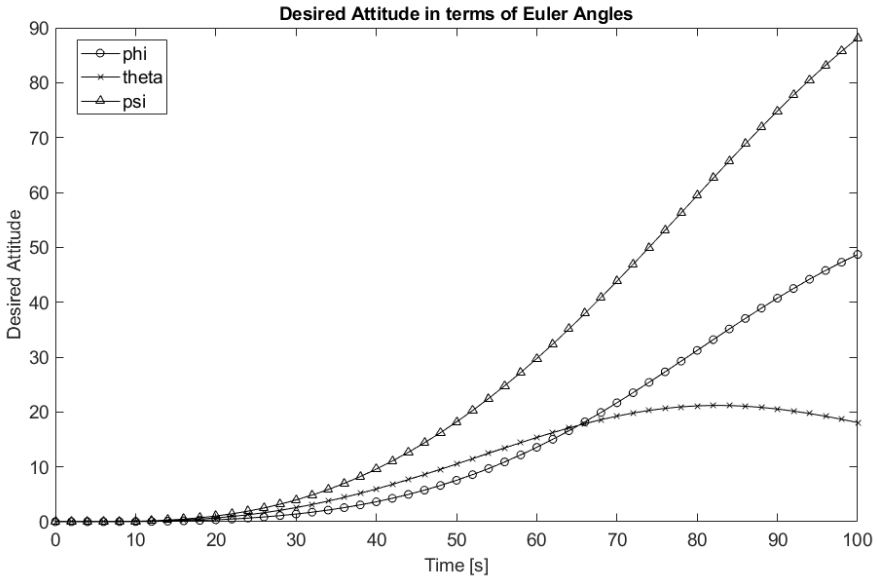

Figure 5.2 Time History of Desired Attitude in terms of Euler Angles

In the simulations, the flexible spacecraft is assumed to have only four bending modes. In Table 5.2, natural frequency and damping ratio of the related modes are given [16].

Table 5.2 Parameters of Flexible Spacecraft

	Natural Frequency(rad/s)	**Damping**
Mode 1	0.7681	0.005607
Mode 2	1.1038	0.00862
Mode 3	1.8733	0.01283
Mode 4	2.5496	0.02516

The characteristics of the piezoelectric are summarized by the piezoelectric charge constant c_p, the Young modulus of elasticity E_p, and the thickness b_p, are listed in Table 5.3 along with the bounding layer parameters. The length, width and thickness of the flexible panel are l, l_a, l_b, respectively. The bending moment M_p due to piezoelectric films is proportional to the applied voltage according to $M_p = -c_p u_p$ with [28]

$$c_p = c_p l_a E_p \frac{E_b b_b (b_p + b_b) + E l_b (b_p + 2b_b + l_b)}{2(E_p b_p + E_b b_b + E l_b)} \text{ Nm/V} \qquad (5.1)$$

Table 5.3 Characteristics of the Piezoelectric Layers of the Flexible Panel

Piezoelectric Layer	**Flexible Panel**
$c_p = 171\times10^{-12}\,\text{m}$	$l = 5\,\text{m}$
$E_p = 139\times10^{9}\ \text{N/m}^2$	$l_a = 0.8\,\text{m}$
$b_p = 2.1\times10^{-3}\,\text{m}$	$l_b = 0.1\,\text{m}$
	$E = 6.8\times10^{10}\,\text{N/m}^2$

Rigid body inertia matrix, coupling matrices and controller parameters are also given in Table 5.4 [16]. The feedback gains $k_p = 1000$, $k_d = 1000$.

Table 5.4 Simulation Parameters used for Controller and Flexible Spacecraft Model

Parameter	**Value**
Control Parameters	$k_p = 1000$ $k_d = 1000$
Piezoelectric Actuator Control Parameters	$\Lambda_1 = 100$ $\Lambda_2 = 100$
Rigid Part Moment of Inertia	$J_{mb} = \begin{bmatrix} 350 & 3 & 4 \\ 3 & 280 & 10 \\ 4 & 10 & 190 \end{bmatrix} kgm^2$
Coupling Matrix between Flexible and Rigid Dynamics	$H = \begin{bmatrix} 6.45637 & 1.27814 & 2.15629 \\ -1.25619 & 0.91756 & -1.67264 \\ 1.11687 & 2.48901 & -0.83674 \\ 1.23637 & -2.6581 & -1.12503 \end{bmatrix} \sqrt{kg}m/s^2$
Coupling Matrix between Flexible Dynamics and Piezoelectric Actuators	$H_2 = \begin{bmatrix} 2.3425\times10^{-2} \\ -4.2253\times10^{-3} \\ 3.9129\times10^{-2} \\ 7.0261\times10^{-2} \end{bmatrix} \sqrt{kg}m/Vs^2$

On the other hand, when piezoelectric actuators are present and chosen as shown in Table 5.4, they increase the stiffness and the internal damping of the system.

Piezoelectric actuators control feedback gain values Λ_1, Λ_2 are selected so that eigenvalues of the dynamics of the bending modes have natural frequencies $\omega_0 = [0.7988 \quad 1.1045 \quad 1.9078 \quad 2.6497]^T$ while for damping $\zeta_0 = [0.009 \quad 0.012 \quad 0.018 \quad 0.152]^T$. Therefore, one has $\Lambda_1 = 100$, $\Lambda_2 = 100$.

All throughout this thesis, attitude control using to-go quaternion is named as classical attitude controller, while attitude controller using to-go quaternion with derivative named as tracking attitude controller.

The effect of tracking controller in spacecraft attitude tracking may be shown by subtracting the quaternion parameters from desired and realized attitude. Without flexible body effects on the spacecraft, it is easy to show the effect of tracking controller on the attitude tracking. Considering only rigid spacecraft dynamics, simulations are performed for classical and tracking attitude controller. In Figure 5.3, component wise difference between desired and realized attitude for classical attitude controller is given. Same graph for tracking attitude controller can be seen in Figure 5.4. Comparing Figure 5.3 and Figure 5.4, it may easily be observed that tracking controller tracks the desired trajectory better than the classical one. This is because of the fact that tracking attitude controller takes the time derivative of the desired attitude into account.

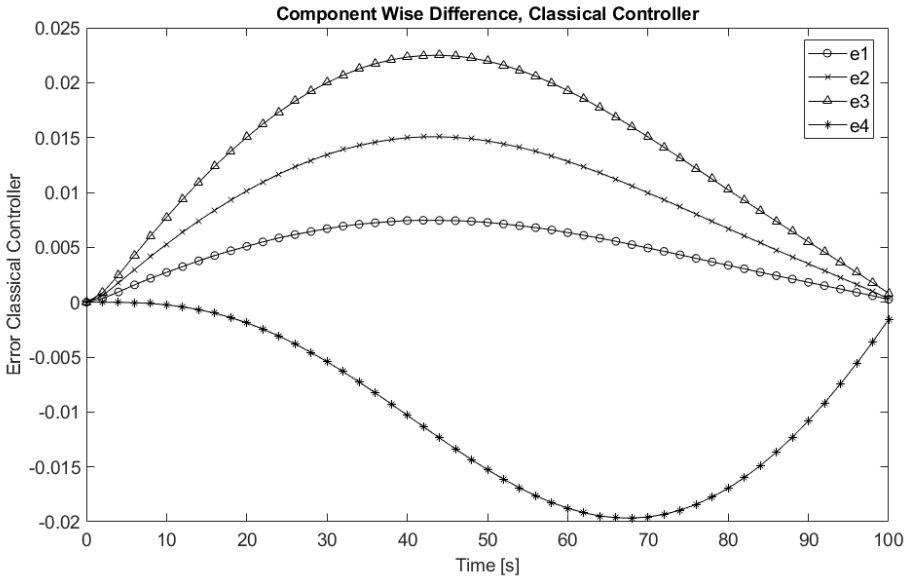

Figure 5.3 Component Wise Difference Between Desired and Realized Quaternion with Classical Controller Only Rigid Body Dynamics Simulated

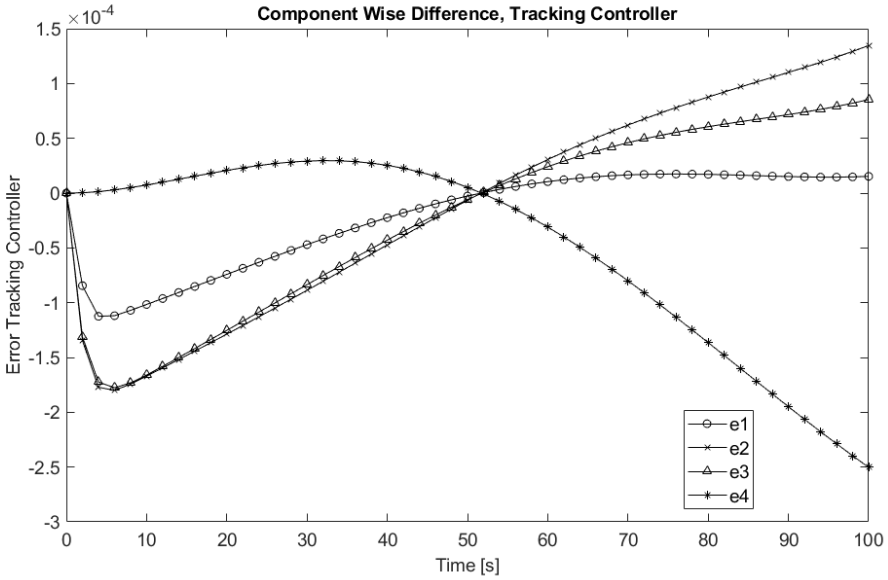

Figure 5.4 Component Wise Difference Between Desired and Realized Quaternion with Tracking Attitude Controller

5.1. Simulation: Case Study 1

In this section, feedback controllers that were developed in Section 4.1, are tested against nonlinear simulations. In the first part, the effect of flexible dynamics is canceled applying a first order low pass filter on the angular velocity measurement of the spacecraft.

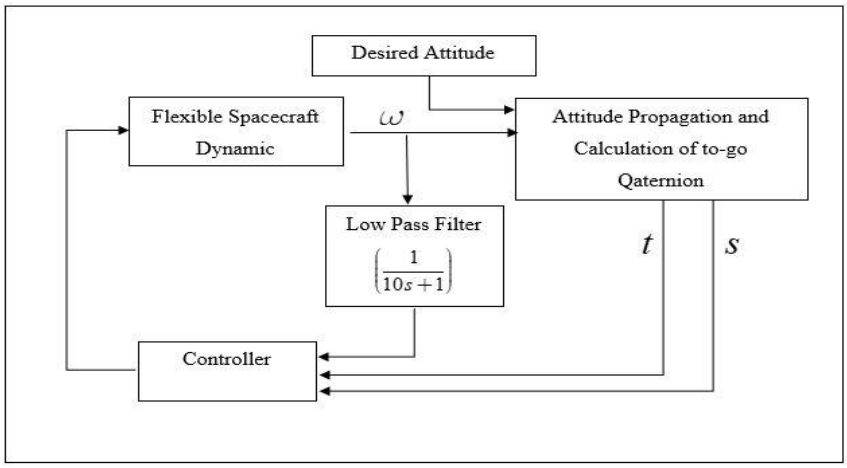

Figure 5.5 Schematic Drawing of Simulation with Low Pass Filter

The effects of flexible dynamics on the pointing accuracy while using low pass filtered and unfiltered measurements is showed comparing body angular velocities and control torques.

5.1.1. Filtered Case

Considering the natural frequencies of the flexible system (Table 5.2), a first order low pass filter is chosen as $\left(\frac{1}{10s+1}\right)$. Then, using tracking attitude controller, time history of body angular velocity may be seen in Figure 5.6.

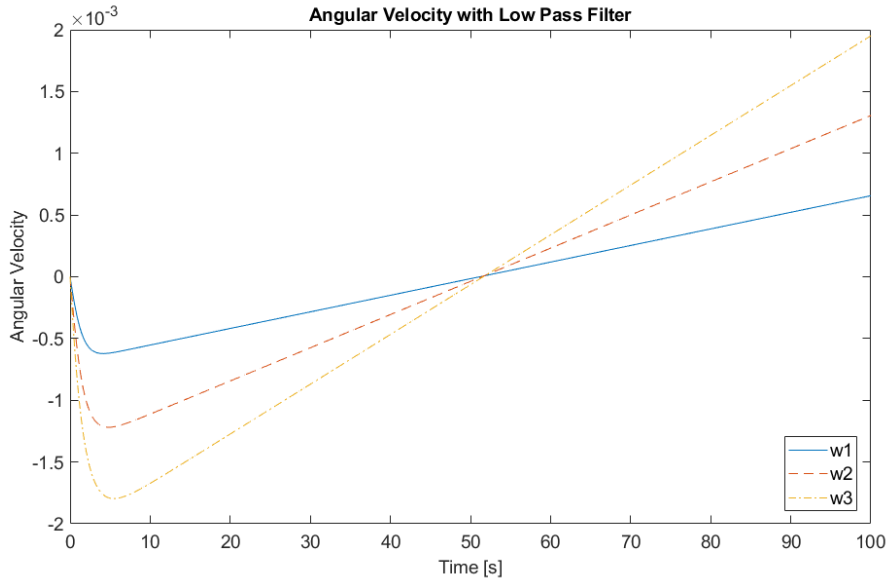

Figure 5.6 Time History of Angular Velocity after Low Pass Filter

Also, corresponding control torque history is presented in Figure 5.7.

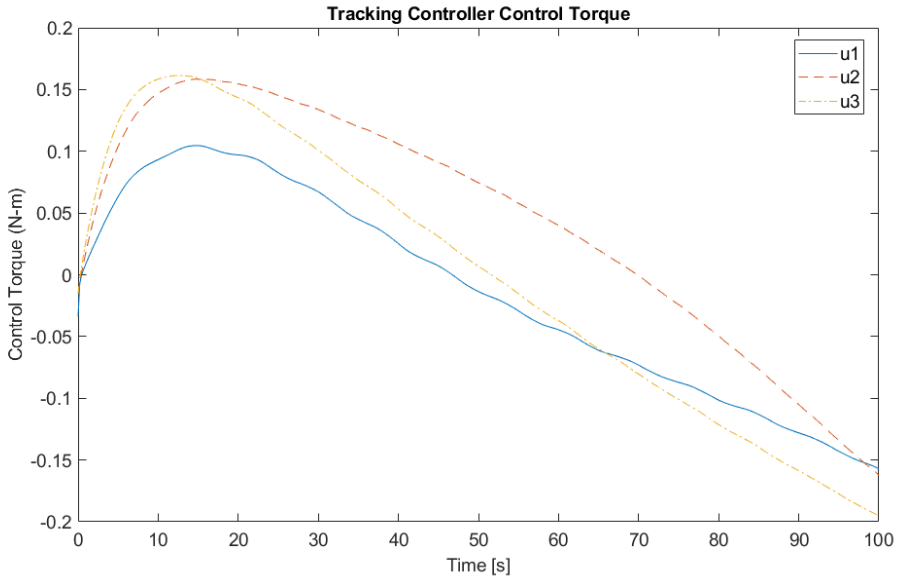

Figure 5.7 Time history of Tracking Controller Control Torque with Low Pass Filter

5.1.2. Non-filtered Case

Simulations are performed this time for the non-filtered case. Using tracking attitude controller, time history of body angular velocity may be observed in Figure 5.8.

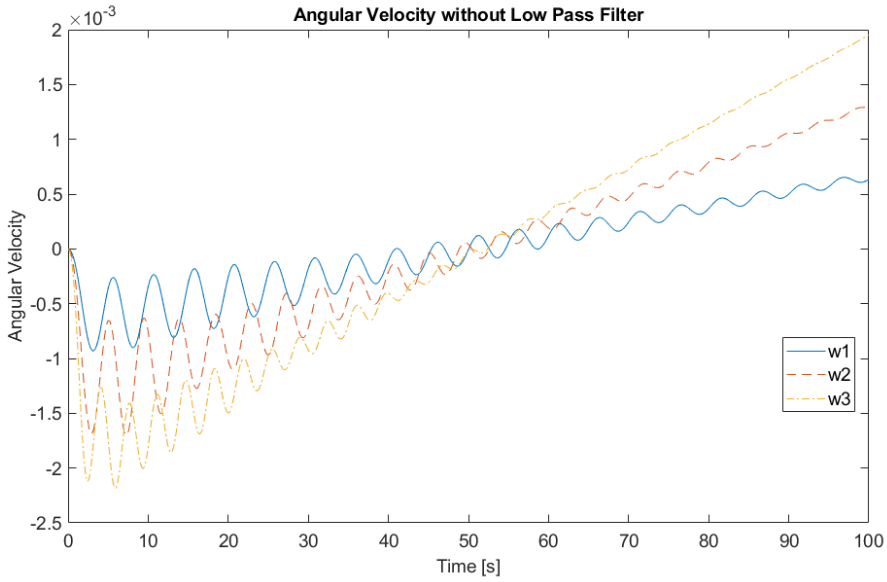

Figure 5.8 Time History of Angular Velocity Without Filter

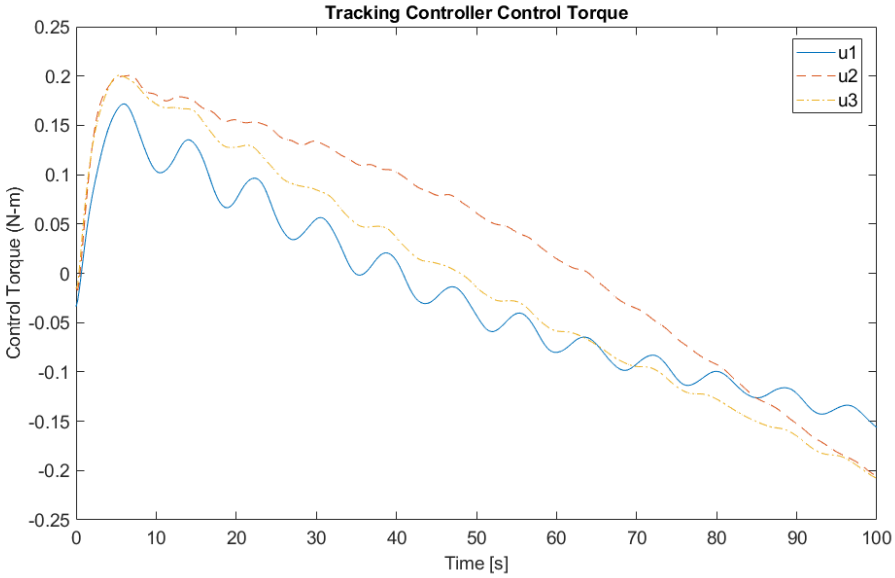

Figure 5.9 Time history of Tracking Controller Control Torque Without Low Pass Filter

Also, Figure 5.9 shows control torque history of flexible spacecraft without filter. Comparing the figures in terms of angular velocities and control torques, it is easily can be said that flexible parts on the spacecraft create oscillations.

To compare tracking attitude controller with the classical one, time history of control torque for classical attitude controller is presented in Figure 5.10. Related controller was given in Section 4.1.2.

Time history of control torque for tracking attitude controller was given in Figure 5.9. Related controller was presented in Section 4.1.3. Comparing Figure 5.9 and Figure 5.10, it can be said that their control torque histories and control torque levels are similar.

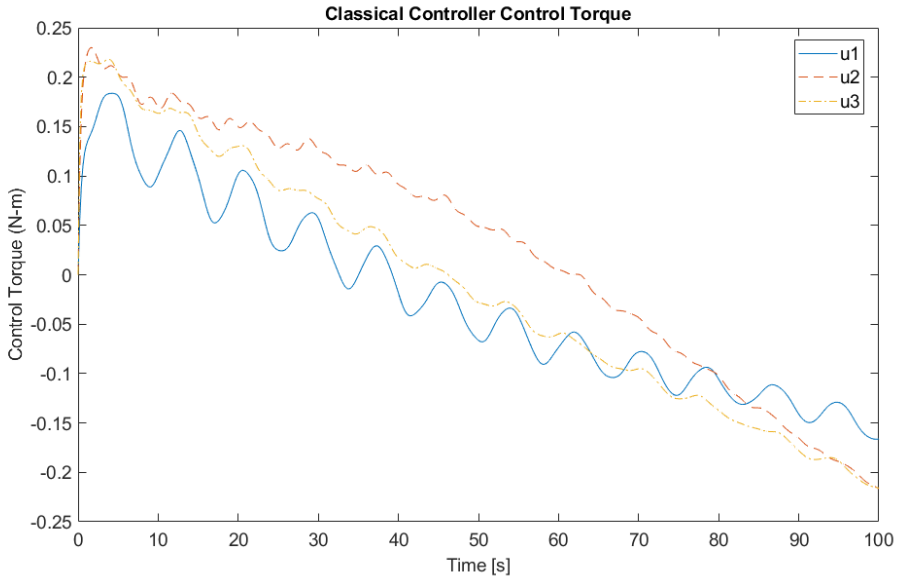

Figure 5.10 Time history of Classical Controller Control Torque Without Filter

5.2. Simulation: Case Study 2

In this section, simulation is performed assuming that flexible body sensors are available and the flexible body dynamics is known. In Section 4.2, the associated formulation was given.

Classical attitude controller was given in Section 4.2.1. Generated vibration energy on the spacecraft using this controller may be observed in Figure 5.11.

Using the tracking controller given in Section 4.2.2, vibration energy graph also may be seen in Figure 5.12. As it may be observed from this figure, using tracking controller the generated total vibration energy is decreased by about 20% as compared to the classical controller. The simulation results show that the success of tracking algorithm to suppress the vibration effects on the spacecraft while using almost the same amount of control torque.

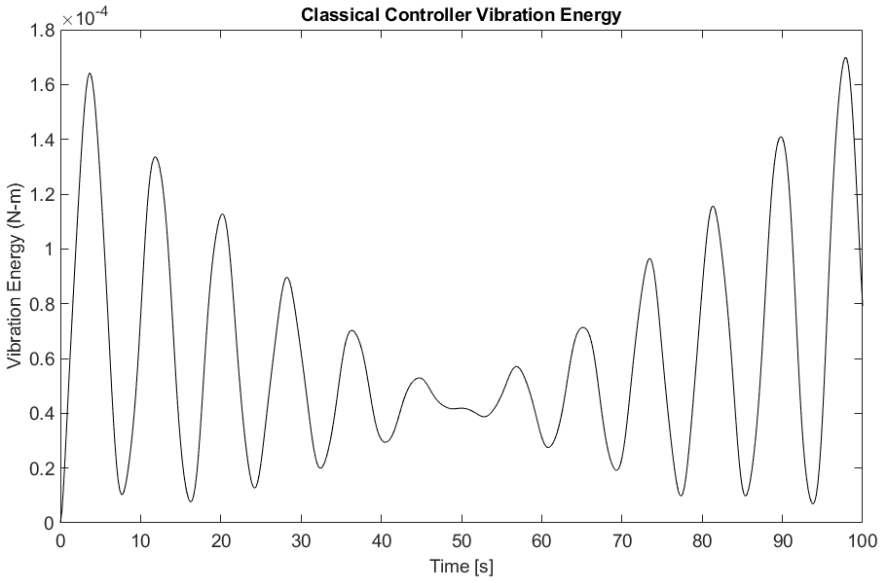

Figure 5.11 Time history of the Vibration Energy with Classical Controller

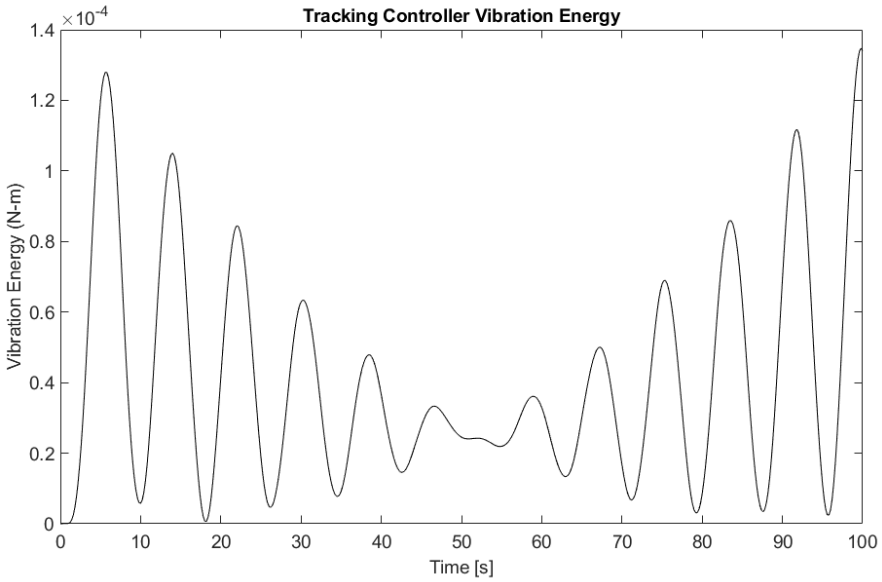

Figure 5.12 Time history of the Vibration Energy with Tracking Controller

5.3. Simulation: Case Study 3

In this section, simulation is performed by adding piezoelectric actuators to the system. Using the controller in Section 4.3.1, the generated vibration energy is presented in Figure 5.13. Also, control torque created by piezoelectric actuators may be seen in Figure 5.14. Comparing Figure 5.13 with Figure 5.11, it may be observed that vibration energy on the spacecraft system is decreased considerably and it is damped out much faster with the help of flexible body torquers as expected.

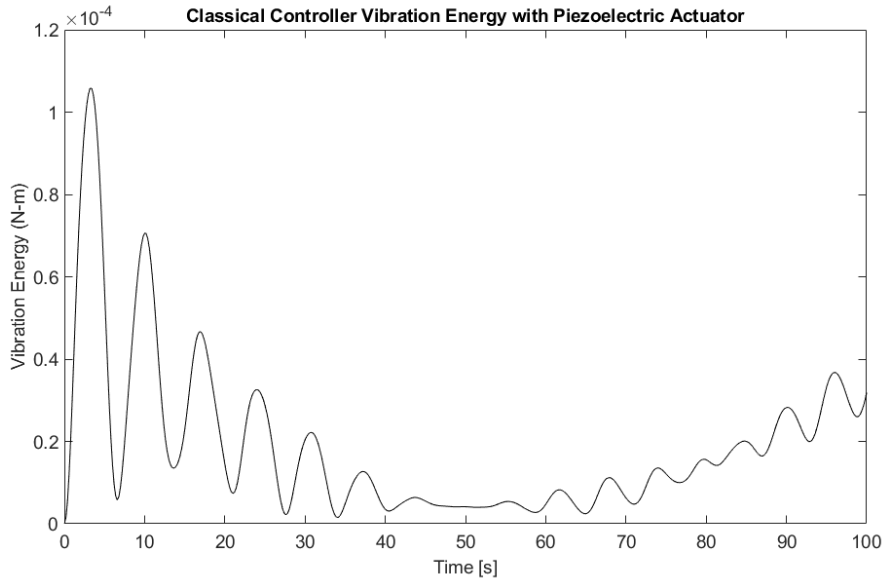

Figure 5.13 Time History of Classical Controller Vibration Energy with Piezoelectric Actuator

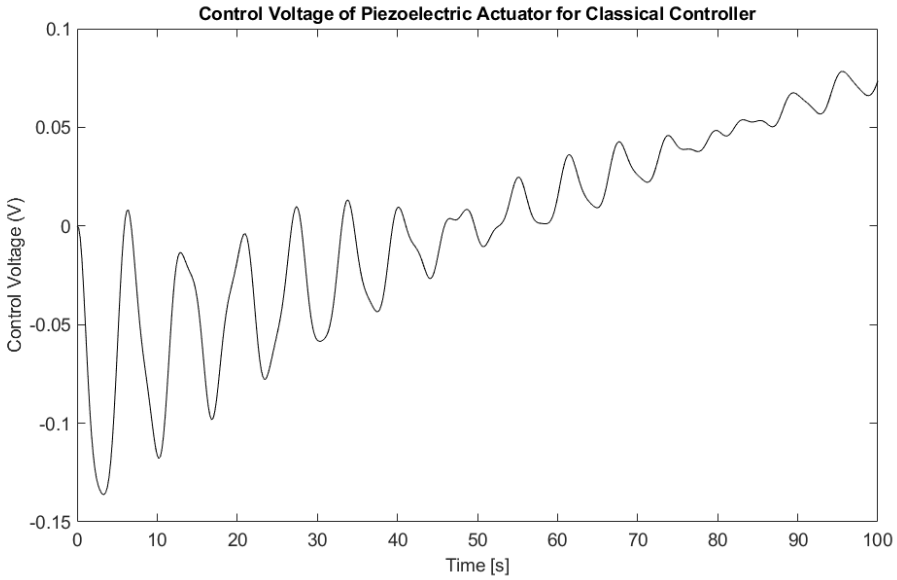

Figure 5.14 Time history of Control Voltage of Piezoelectric Actuator for Classical Controller

Using the controller given in Section 4.3.2, graph of vibration energy on the system is presented in Figure 5.15. The graph shows that with piezoelectric actuators and tracking controller, vibration energy is reduced by about 30%. Thus, the best solution

for the vibration problem is obtained using tracking attitude controller and adding piezoelectric actuators to the system. Moreover, as it may be observed from Figure 5.16, tracking controller needs much more less firing on the piezoelectric control voltages.

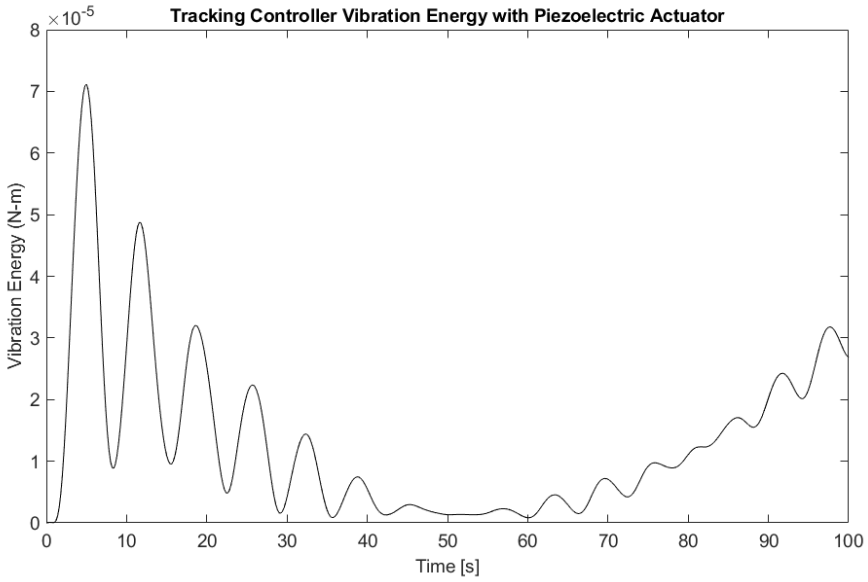

Figure 5.15 Time History of Tracking Controller Vibration Energy with Piezoelectric Actuator

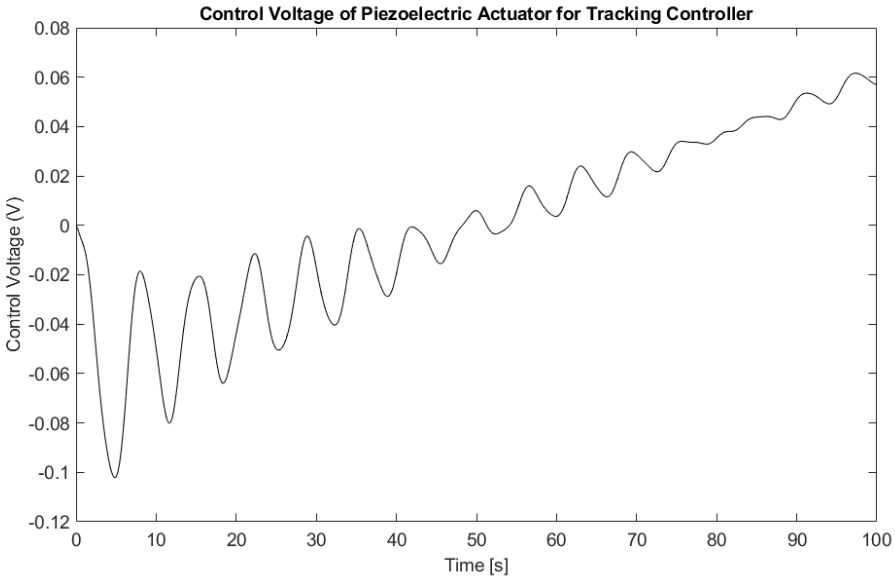

Figure 5.16 Time history of Control Voltage of Piezoelectric Actuator for Tracking Controller

CHAPTER 6

CONCLUSION AND FUTURE WORK

In this thesis, flexible spacecraft vibration suppression, using a time dependent to-go quaternion formulation as attitude propagator, is examined. A feedback control algorithm is obtained with the help of Lyapunov's direct method. A classical PD-like controller is obtained by using attitude controller that contains time dependent trajectory. After that, recently developed attitude controller that takes into account time dependent trajectory and its derivative, is used to obtain tracking control law. Obtained tracking controller is different from the PD-like controller due to the new term in control torque. Tracking controller provides us with more precise and smoother trajectory tracking. That also means that vibration effect in the flexible spacecraft decreased in attitude tracking missions. Also, tracking controller is almost same control torque histories and levels with the classical PD-like controller.

In the first case, controller is derived using unmodeled dynamics. Applying first order low pass filter on angular velocity, the effect of flexible parts on the spacecraft is shown. It effects both body angular velocity and control torque. Body angular velocity is important for pointing accuracy. On the other hand, control torque that is applied is very important because fuel consumption in the space is very limited. Also, obtained controller in the first case may be used as a controller in any failure in the discrete flexible body sensors and discrete flexible body torquers. Although its performance is lower, it is preferable on the grounds that it can be superior to the sensor redundancy policy because it is only based on extra software capabilities on the on-board computer.

Second controller is obtained considering spacecraft have discrete flexible body sensors as well as rigid body sensors. In this controller, only rigid body actuators are considered. Controller is developed for both attitude controllers. The success of

tracking algorithm to suppress the vibration effects on the spacecraft is shown by comparing with the classical controller. Also, in any case of failure in the flexible body torquers, second controllers can be used as a controller for the spacecraft.

Another controller is designed based on the spacecraft system that contains piezoelectric actuator in the system. Piezoelectric actuators provide increasing stiffness and internal damping for the system. Simulation results show that tracking controller with piezoelectric actuator was more successful in the attenuation of flexible effects compared to classical PD-like controller. It is observed that, when attitude trajectory mission is defined, almost half of the vibration effect on the spacecraft system decreased with the help of tracking controller.

In the future, better positioning of piezoelectric actuators on real satellite structures shall be carried out. In addition, the effects of using reduced order flexible structure models on actual satellite structures shall also be investigated.

REFERENCES

[1] J. Vago, B. Gardini, P. Baglioni, G. Kminek, G. Gianfiglio and E. Project Team, "Science objectives of ESA's ExoMars mission," 2018.

[2] A. Baz and S. Poh, "Performance of an Active Control System with Piezoelectric Actuators," *Journal of Sound and Vibration,* vol. 126, no. 2, pp. 327-343, 1988.

[3] Z. Li and P. M. Bainum, "Vibration Control of Flexible Spacecraft Integrating a Momentum Exchange Controller and a Distributed Piezoelectric Actuator," *Journal of Sound and Vibration,* vol. 177, no. 4, pp. 539-553, 1994.

[4] D. C. Hyland, J. L. Junkins and R. W. Longman, "Active Control Technology for Large Space Structures," *Journal of Guidance, Control, and Dynamics,* vol. 16, no. 5, pp. 801-821, 1993.

[5] E. F. Crawley and J. De Luis, "Use of Piezoelectric Actuators as Elements of Intelligent Structures," *AIAA Journal,* vol. 25, no. 10, pp. 1373-1385, 1987.

[6] S. M. Yang and Y. J. Lee, "Modal Analysis of Stepped Beams with Piezoelectric Materials," *Journal of Sound and Vibration,* vol. 176, no. 3, pp. 289-300, 1994.

[7] M. Sidi, Spacecraft Dynamics and Control: A Practical Engineering Approach, Cambridge : Cambridge University Press, 1997.

[8] L. Mazzini, Flexible Spacecraft Dynamics Control and Guidance, Rome: Springer, 2016.

[9] C. Zhong, Y. Gou, Z. Yu and Q. Chen, "Finite-time attitude control," *Transactions of the Institute of Measurement and Control,* vol. 38, no. 2, pp. 240-249, 2016.

[10] J. J. Kim and B. N. Agrawal, "Experiments on Jerk-Limited Slew Maneuvers of a," in *AIAA Guidance, Navigation, and Control Conference and Exhibit*, Colorado, 2006.

[11] J. J. Kim and B. N. Agrawal, "Rest-to-Rest Slew Maneuver of Three-Axis Rotational Flexible Spacecraft," in *17th International Federation of Automatic Control World Congress*, Seoul, 2008.

[12] Q. Hu, Z. Wang and H. Gao, "Sliding Mode and Shaped Input Vibration Control of Flexible Systems," *IEEE Transactions on Aerospace and Electronic Systems*, vol. 44, no. 2, pp. 503-519, 2008.

[13] D. Li and W. Wang, "An Intelligent Sliding Mode Controller for Vibration Supression in Flexible Structures," *Journal of Vibration and Control*, vol. 17, no. 14, pp. 2187-2198, 2011.

[14] H. Bang, C. Ha and J. H. Kim, "Flexible Spacecraft Attitude Maneuver by Application of Sliding Mode Control," *Acta Astronautica*, vol. 57, no. 11, pp. 841-850, 2005.

[15] A. Iyer and S. N. Singh, "Sliding Mode Control of Flexible Spacecraft Under Disturbance Torque," *Proceedings of the 27th IEEE Conference on Decision and Control*, vol. 1, pp. 718-723, 1988.

[16] Q. Hu, "Robust Adaptive Sliding Mode Attitude Control and Vibration Damping of Flexible Spacecraft Subject to Unknown Disturbance and Uncertainity," *Transactions of the Institute of Measurement and Control*, vol. 34, no. 4, pp. 436-447, 2011.

[17] B. Wie, Space Vehicle Dynamics and Control, VA, Reston: AIAA, 1998.

[18] B. Wie, H. Weiss and A. Arapostathis, "Quaternion Feedback Regulator for Spacecraft Eigenaxis Rotation," *Journal of Guidance, Control, and Dynamics*, vol. 12, no. 3, 1989.

[19] L. Meirovitch, Methods of Analytical Dynamics, New York: McGraw-Hill, 1970.

[20] T. A. Dwyer, "Exact Nonlinear Control of Large Angle Rotational Maneuvers," *IEEE Transactions on Automatic Control*, vol. 29, no. 9, pp. 769-774, 1984.

[21] T. A. Dwyer, H. Sira-Ramirez, S. Monaco and S. Stornelli, "Variable Structure Control of Globally Feedback-Decoupled Deformable Vehicle Maneuvers," in *Proceedings of the 26th IEEE Conference on Decision and Control*, Los Angeles, 1987.

[22] S. Monaco and S. Stornelli, "A Nonlinear Feedback Control Law for Attitude Control," in *Algebraic and Geometric Methods in Nonlinear Control Theory*, Rome, 1984, pp. 573-595.

[23] A. M. Annasawmy and D. J. Clancy, "Adaptive Control Strategies for Flexible Space Structures," *IEEE Transactions on Aerospace and Electronic Systems*, vol. 32, no. 3, pp. 952-965, 1996.

[24] S. N. Singh, "Nonlinear Adaptive Attitude Control of Spacecraft," *IEEE Transactions on Aerospace and Electronic Systems*, vol. 23, no. 3, pp. 371-379, 1987.

[25] G. Georgiou, G. S., S. Monaco and D. Normand-Syrot, "On the Nonlinear Adaptive Control of a Flexible Spacecraf," in *Proceedings of the 1st ESA Conference on Spacecraft Guidance,Navigation,and Control Systems*, Noordwijk, 1991.

[26] B. Xiao, Q. Hu and Y. Zhang, "Fault-Tolerant Attitude Control for Flexible Spacecraft Without Angular Velocity Magnitude Measurement," *Journal of Guidance, Control, and Dynamics,* vol. 34, no. 5, pp. 1556-1561, 2011.

[27] Z. Gao, B. Han, M. Qian and J. Zhao, "Active Fault Tolerant Control for Flexible Spacecraft with Sensor Faults Using Adaptive Integral Sliding Mode," in *Chinese Intelligent Automation Conference,* 2018.

[28] S. Gennaro, "Output Stabilization of Flexible Spacecraft with Active Vibration Suppression," *IEEE Transactions on Aerospace and Electronic Systems,* vol. 39, no. 3, pp. 747-759, 2003.

[29] B. Han, Z. Gao, Y. Xu, J. Zhao and T. Cao, "Fault Tolerant Control Design for the Attitude Control Systems of Flexible Spacecraft with Sensor Faults," in *Chinese Control and Decision Conference,* 2016.

[30] Y. Fujisaki, M. Ikeda and K. Miki, "Robust Stabilization of Large Space Structures via Displacement Feedback," *IEEE Transactions on Automatic Control,* vol. 46, no. 12, pp. 1993-1996, 2001.

[31] B. N. Agrawal, "Spacecraft Vibration Suppression Using Smart Structures," in *4th International Congress on Sound and Vibration*, 1996.

[32] J. L. Fanson and T. K. Caughey, "Positive Position Feedback Control for Large Structure," *AIAA Journal,* vol. 28, no. 4, pp. 717-724, 1990.

[33] G. Song, P. S. Schmidt and N. B. Agrawal, "Experimental Robustness Study of Positive Position Feedback Control for Active Vibration Suppression," *Journal of Guidance, Control and Dynamics,* vol. 25, no. 1, pp. 179-182, 2002.

[34] G. Song and B. Kotejoshyer, "Vibraion Reduction of Flexible Structures During Slew Operations," *International Journal of Acoustic and Vibration,* vol. 7, no. 2, pp. 105-109, 2002.

[35] Q. Hu and G. F. Ma, "Variable Structure Control and Active Vibration Suppression of Flexible Spacecraft During Attitude Maneuver," *Aerospace Science and Technology,* vol. 90, pp. 307-317, 2005.

[36] O. Tekinalp, M. M. Gomroki and Ö. Ataş, "Nonlinear Tracking Attitude Control of Spacecraft on Time Dependent Trajectories," in *AAS/AIAA Astrodynamics Specialist Conference* , Colorado, 2015.

[37] O. Tekinalp and A. Tekinalp, "Tracking Control of Spacecraft Attitude on Time Dependent Trajectories," in *AIAA/AAS Astrodynamics Specialist Conference*, California, 2016.

[38] K. Sharmilla, O. Tekinalp and K. Özgören, "Quaternion Based State Dependent Ricatti Equation Control of a Satellite Camera on Piezoelectric Actuators," in *AIAA/AAS Astrodynamics Specialist Conference*, Ontario, 2010.

[39] I. S. Committee, IEEE Standart on Piezoelectricity, New York: Institute of Electrical and Electronics Engineers, 1988.

[40] J. Junkins and Y. Kim, Introduction to Dynamics and Control of Flexible Structures, Washington: American Institute of Aeronautics and Astronautics, 1993.

[41] H. K. Khalil, Nonlinear Systems, New Jersey: Upper Saddle River, 1996.